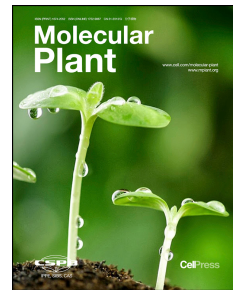


Journal Pre-proof

The Small GTPase RABA2a Recruits SNARE Proteins to Regulate Secretory Pathway in Parallel with the Exocyst Complex in *Arabidopsis*

Lei Pang, Zhiming Ma, Xi Zhang, Yuanzhi Huang, Ruili Li, Yansong Miao, Ruixi Li



PII: S1674-2052(21)00439-1

DOI: <https://doi.org/10.1016/j.molp.2021.11.008>

Reference: MOLP 1272

To appear in: MOLECULAR PLANT

Accepted Date: 12 November 2021

Please cite this article as: **Pang L., Ma Z., Zhang X., Huang Y., Li R., Miao Y., and Li R.** (2021). The Small GTPase RABA2a Recruits SNARE Proteins to Regulate Secretory Pathway in Parallel with the Exocyst Complex in *Arabidopsis*. Mol. Plant. doi: <https://doi.org/10.1016/j.molp.2021.11.008>.

This is a PDF file of an article that has undergone enhancements after acceptance, such as the addition of a cover page and metadata, and formatting for readability, but it is not yet the definitive version of record. This version will undergo additional copyediting, typesetting and review before it is published in its final form, but we are providing this version to give early visibility of the article. Please note that, during the production process, errors may be discovered which could affect the content, and all legal disclaimers that apply to the journal pertain.

© 2021 The Author

1 **The Small GTPase RABA2a Recruits SNARE Proteins to Regulate Secretory**
2 **Pathway in Parallel with the Exocyst Complex in *Arabidopsis***

3

4 Lei Pang¹, Zhiming Ma², Xi Zhang³, Yuanzhi Huang¹, Ruili Li³, Yansong Miao² and
5 Ruixi Li^{1*}

6 1. Key Laboratory of Molecular Design for Plant Cell Factory of Guangdong Higher
7 Education Institutes, Institute of Plant and Food Science, School of Life Sciences,

8 Southern University of Science and Technology, Shenzhen 518055, China

9 2. School of Biological Sciences, Nanyang Technological University, Singapore
10 637551, Singapore

11 3. College of Biological Sciences and Technology, Beijing Forestry University, Beijing
12 100083, China

13

14 **Running title:** RABA2a regulates the secretory pathway

15

16 **Email addresses of authors:**

17 Lei Pang: pangl@sustech.edu.cn

18 Zhiming Ma: zhiming.ma@ntu.edu.sg

19 Xi Zhang: zhangxi@bjfu.edu.cn

20 Yuanzhi Huang: 11930164@mail.sustech.edu.cn

21 Ruili Li: liruili@bjfu.edu.cn

22 Yansong Miao: yansongm@ntu.edu.sg

23 Ruixi Li: lirx@sustech.edu.cn

24

25 *** To whom correspondence should be addressed:**

26 Ruixi Li: lirx@sustech.edu.cn

27 Key Laboratory of Molecular Design for Plant Cell Factory of Guangdong Higher
28 Education Institutes, Institute of Plant and Food Science, School of Life Sciences,
29 Southern University of Science and Technology, Shenzhen 518055, China.

30

31 SHORT SUMMARY

32 Classic cell biology studies suggest that the exocyst is required to anchor secretory
33 vesicles to the PM prior to SNARE complex-mediated membrane fusion. In this study,
34 we unexpectedly find that the small GTPase RABA2a interacts with the SNARE
35 complex for membrane fusion bypass the exocyst. We provide multiple lines of
36 evidence that the RABA2a-SNARE- and exocyst-mediated secretory pathways are
37 largely independent.

38 ABSTRACT

40 Delivery of proteins to the plasma membrane occurs via secretion, which requires
41 tethering, docking, priming, and fusion of vesicles. In yeast and mammalian cells, an
42 evolutionarily conserved RAB GTPase activation cascade functions together with the
43 exocyst and SNARE proteins to coordinate vesicle transport with fusion at the plasma
44 membrane. However, whether this is the case in plants is unclear. In this study, we show
45 that the small GTPase RABA2a recruits and interacts with the VAMP721/722-SYP121-
46 SNAP33 SNARE ternary complex for membrane fusion. We also demonstrate that both
47 RABA2a and the downstream SNARE proteins do not interact with the exocyst
48 subunits. RABA2a inactivation does not affect the subcellular localization or assembly
49 of the exocyst, and the mutation of exocyst subunit does not disrupt the RABA2a-
50 SNARE association or SNARE assembly. Therefore, the RABA2a-SNARE- and
51 exocyst-mediated secretory pathways are largely independent. Live videos reveal that
52 the two sets of proteins follow non-overlapping trafficking routes. Genetic evidence
53 support that the two pathways select different cargos. Finally, we demonstrate that the
54 plant-specific RABA2a-SNARE pathway is essential to maintain potassium
55 homeostasis. Our findings imply that highly conserved endomembrane proteins
56 develop plant-specific trafficking mechanisms to accommodate the changing
57 environment.

58
59 **Keywords:** exocyst, RABA2a, secretory process, SNARE complex

61 INTRODUCTION

62 The secretory pathway is essential for proper cellular function during growth and
 63 stress responses. Newly synthesized proteins are initially targeted to the endoplasmic
 64 reticulum (ER) and then delivered to the Golgi apparatus for modification (Rosquete et
 65 al., 2018). Cargo proteins from endocytic or biosynthetic pathways meet at the trans-
 66 Golgi network (TGN) for further sorting. After sorting, ADP ribosylation factor (ARF)
 67 GTPases, RAB GTPases, and SNARE (soluble N-ethylmaleimide sensitive factor
 68 attachment protein receptor) proteins coordinately regulate vesicle budding and
 69 membrane fusion (Nielsen et al., 2008; Wu et al., 2008). One of the best-characterized
 70 functions of RAB GTPases is vesicle tethering and membrane fusion. Following their
 71 activation by guanine nucleotide exchange factors (GEFs), GTP-bound RABs facilitate
 72 the membrane recruitment of tethering factors, including long coiled-coil proteins and
 73 multi-subunit protein complexes (Gerdes, 2008; Stenmark, 2009). The exocyst is an
 74 evolutionarily conserved tethering complex consisting of eight subunits: Secretory3
 75 (Sec3), Sec5, Sec6, Sec8, Sec10, Sec15, Exocyst70 (Exo70), and Exo84 (Heider and
 76 Munson, 2012; Liu and Guo, 2012). The exocyst complex directs vesicles to the plasma
 77 membrane (PM) via membrane tethering prior to SNARE protein-mediated fusion (He
 78 and Guo, 2009; He et al., 2007).

79 In yeast and mammalian cells, an evolutionarily conserved pathway functions in
 80 secretory processes. In yeast, Yeast Protein Two 31 (Ypt31) and its homolog Ypt32
 81 recruit Sec2p after their activation by upstream GEFs. Sec2p is also a GEF and
 82 subsequently activates the downstream protein Sec4p during polarized transport (Ortiz
 83 et al., 2002). Activated Sec4p mediates the recruitment of the exocyst to secretory
 84 vesicles and the assembly of the exocyst complex by interacting with subunit Sec15
 85 (Guo et al., 1999; Luo et al., 2014). The mammalian homologs of Sec4p, Sec2p, and
 86 Ypt31/32p are Rab8, Rabin8, and Rab11, respectively. During primary ciliogenesis,
 87 activated Rab11 interacts with Rabin8 and kinetically stimulates its guanine nucleotide
 88 exchange activity towards Rab8 (Das and Guo, 2011; Knodler et al., 2010). The exocyst
 89 subunit Sec15 directly interacts with GTP-bound Rab8 or Rab11 (Oztan et al., 2007;
 90 Zhang et al., 2004). Thus, a Rab GTPase activation cascade, together with the exocyst

91 complex, couples the generation of secretory vesicles at donor compartments with their
 92 docking and fusion at the PM (Das and Guo, 2011). All the components of this secretory
 93 pathway are present in plants. However, whether this conserved mechanism functions
 94 in plants during the secretory process remains unclear.

95 The secretory pathway is conserved in plants but differs from that in yeast and
 96 mammals. The Rab11 family is expanded in plants, with 26 RABA paralogs divided
 97 into six subclades: RABA1 to RABA6. Different RABA GTPases define separate TGN
 98 sorting compartments (Rutherford and Moore, 2002; Vernoud et al., 2003). RABA2 and
 99 RABA3 label a TGN domain that controls cargo delivery to the cell plate during
 100 cytokinesis (Chow et al., 2008). This unique TGN subdomain is distinct from the
 101 SYNTAXIN OF PLANTS 61 (SYP61)-labeled TGN domain, to which RABA4b
 102 preferentially localizes and which is responsible for the transport of cell wall
 103 components (Preuss et al., 2006). The exocyst complex in the model plant *Arabidopsis*
 104 *thaliana* (hereafter *Arabidopsis*) contains all the subunits present in other eukaryotic
 105 systems (Chong et al., 2010). However, whereas the exocyst subunits in yeast and
 106 mammals are encoded by single-copy genes, the plant SEC3, SEC5, SEC10, and
 107 SEC15 subunits are encoded by two genes, EXO84 by three genes, and EXO70 by as
 108 many as 23 genes. The functional diversification of different EXO70s has been widely
 109 characterized. Plant EXO70 paralogs are involved in processes such as cytokinesis,
 110 pollen tube growth, root hair elongation, callose deposition, and defense responses
 111 (Pecenkova et al., 2011; Synek et al., 2006; Synek et al., 2017; Zhao et al., 2015). The
 112 unique EXO70 paralog EXO70B1 helps regulate the autophagy-related membrane
 113 transport pathway from the ER to the vacuole, which bypasses the Golgi apparatus
 114 (Kulich et al., 2013). The Exo70B2 isoform is recently reported to transport to the
 115 vacuole after autophagy induction by immunogenic peptide flg22 (Brillada et al., 2021).
 116 A novel double-membrane compartment named the exocyst-positive organelle (EXPO)
 117 is characterized by the presence of the EXO70 paralog EXO70E2 (Lin et al., 2015;
 118 Wang et al., 2010). EXPOs are different from autophagosomes because 1) their
 119 formation is not induced by starvation; 2) they do not fuse with lytic compartments;
 120 and 3) they do not colocalize with the autophagosome marker AUTOPHAGY-

121 RELATED PROTEIN 8e (ATG8e). Although the origin and mechanism of formation
 122 of EXPOs are unknown, they are thought to sequester and transport leaderless proteins
 123 to the extracellular space (Ding et al., 2014; Wang et al., 2017). Therefore, the exocyst
 124 complex in land plants includes highly diverse isoforms with different functions and/or
 125 roles in different biological processes.

126 Although many studies have aimed to independently characterize the functions of
 127 RABA GTPases or exocyst subunits (Berson et al., 2014; Choi et al., 2013; Fendrych
 128 et al., 2013; Feraru et al., 2012; Hala et al., 2008; Stegmann et al., 2012; Szumlanski
 129 and Nielsen, 2009; Vukasinovic and Zarsky, 2016; Wang *et al.*, 2010), the connection
 130 between the two sets of proteins is unclear. The expansion of RABA and EXO70
 131 paralogs in plants has likely increased their complexity. STOMATAL CYTOKINESIS
 132 DEFECTIVE1 (SCD1) and SCD2 proteins contain the conserved DENN (differentially
 133 expressed in normal and neoplastic cells) domain, similar to Sec2p in yeast and Rabin8
 134 in mammals. These proteins directly interact with both RABE1 GTPases (paralogs of
 135 Sec4 or Rab8) and SEC15b in plants (Mayers et al., 2017), suggesting that the secretory
 136 pathway in other eukaryotic systems is partially conserved in plants. However, whether
 137 RAB activation cascades also exist in plants remains unclear.

138 Here, we investigated the mechanism of the RABA2a-regulated secretory pathway.
 139 Through immunoprecipitation (IP) coupled with mass spectrometry (MS) and further
 140 evaluation, we demonstrate that the SNARE proteins VESICLE-ASSOCIATED
 141 MEMBRANE PROTEIN 721 (VAMP721) and SYP121 are the downstream effectors
 142 of the small GTPase RABA2a. The RABA2a-regulated secretory pathway bypasses
 143 RABE1 GTPases and the exocyst but directly interacts with SNARE proteins.
 144 Biochemical, genetic, and cell biology experiments revealed that the RABA2a-
 145 SNARE- and exocyst-mediated secretory pathways are largely independent, with
 146 different trafficking routes and different cargos. Our results suggest that plants have
 147 generated different endomembrane sorting pathways during evolution and provide
 148 important insights into a plant-specific mechanism for the secretory process.

149

150 **RESULTS**

151 **The SNARE proteins VAMP721 and SYP121 are the downstream effectors of**
 152 **RABA2a**

153 The small RAB GTPase RABA2a localizes to subdomains of the TGN and
 154 regulates vesicle trafficking from the TGN to the PM (Chow *et al.*, 2008). We recently
 155 reported that constitutive accumulation of a dominant negative form of RABA2a
 156 selectively diminishes the secretion and recycling of non-basal PM proteins (Li *et al.*,
 157 2017b). To unravel the molecular and cellular mechanisms of the RABA2a-regulated
 158 secretory pathway, we explored the interactors of RabA2A by IP and MS analysis. The
 159 SNARE proteins VAMP721 and SYP121, among the top hits, drew our attention. We
 160 chose to study the SNARE proteins in detail, as they form the SNARE complex in
 161 response to pathogen infection and play essential roles in secretory pathways (Kwon *et*
 162 *al.*, 2008).

163 First, we validated the interaction between RABA2a and SNARE proteins by co-
 164 IP. We generated two antibodies that recognize VAMP721 or SYP121 (**Supplemental**
 165 **Figure 1A and 1B**), although we cannot exclude the possibility that they may also
 166 recognize the closest homologs of these proteins, VAMP722 and SYP122, respectively.
 167 Both VAMP721 and SYP121 co-immunoprecipitated with YFP-RABA2a (**Figure 1A**),
 168 consistent with the MS data. By contrast, we failed to detect the two other RAB
 169 GTPases RABC1 and RABD2b by co-IP, although they are also in the secretory
 170 pathway (**Figure 1A**) (Peng *et al.*, 2011; Pinheiro *et al.*, 2009; Rutherford and Moore,
 171 2002).

172 We further confirmed the interaction by split-ubiquitin yeast two-hybrid (SU-Y2H)
 173 analysis, as both SNARE proteins contain a transmembrane domain (TMD) at their C
 174 termini. RAB GTPases are lipid-modified through the two cysteine residues at their C
 175 termini for membrane targeting (Pereira-Leal *et al.*, 2001). To eliminate the possibility
 176 of false-positive results from membrane targeting, we deleted the last five amino acids
 177 (ΔC) containing the cysteine residues at the C termini of RAB GTPases in all the
 178 following interaction assays as previously described (Antignani *et al.*, 2015; Preuss *et*
 179 *al.*, 2006). Co-transformation of constructs for RABA2a ΔC and VAMP721 or SYP121
 180 supported yeast growth on medium lacking His, Leu, and Trp and containing 3-AT for

high stringency (**Figure 1B and 1C**), indicating that both SNARE proteins interact with RABA2a. The interaction was specific for the GTP-bound active state, since the two SNARE proteins interacted with both wild-type and constitutively active mutant RABA2a(Q71L)ΔC, but not with the constitutively inactive mutant RABA2a(S26N)ΔC (**Figure 1B and 1C**), which is predicted to bind to GDP (Chow *et al.*, 2008). Since VAMP721 belongs to the VAMP72 clade and SYP121 belongs to the SYP12 clade, we further examined whether the homologous proteins interacted with RABA2a. Here we showed that both VAMP722 and SYP122 interacted with GTP-bound RABA2a. On the contrary, VAMP723, VAMP726 and VAMP727, the close homologs of VAMP721, and SYP123, SYP124 and SYP125, the close homologs of SYP121, failed to interact with active RABA2a (**Figure 1D and 1E**). We confirmed that the lack of interaction was not caused by lack of accumulation of prey or bait proteins (**Supplemental Figure 2A-2J**). Overall, these results suggest that RABA2a selectively interacts with some members of SNARE proteins from VAMP72 and SYP12 clades in its GTP-bound state.

We then performed a luciferase complementation imaging (LCI) experiment via transient infiltration in *Nicotiana benthamiana* leaves. In accordance with the results of SU-Y2H, VAMP721 and SYP121 exhibited strong luciferase activity with RABA2a(Q71L)ΔC but much weaker signals with RABA2a(S26N)ΔC (**Supplemental Figure 3A and 3B**). VAMP722 and SYP122 also interacted with RABA2a(Q71L)ΔC in LCI assays (**Supplemental Figure 3C and 3D**). By contrast, no significant luciferase signal was observed when VAMP723, VAMP726, SYP123, SYP124, and SYP125 were combined with RABA2a(Q71L)ΔC (**Supplemental Figure 3C and 3D**).

To provide additional support to these results, we performed a bimolecular fluorescence complementation (BiFC) assay in *N. benthamiana* leaf epidermal cells. We used the 2in1 cloning system, which contains an internal expression control (*RFP*) within a single vector to ensure a 1:1 expression ratio of the *nYFP* and *cYFP* halves and enables ratiometric analysis of the interaction partners (**Figure 1F and 1G**) (Grefen and Blatt, 2012; Karnik *et al.*, 2013). We detected strong fluorescence from reconstituted YFP in cells coexpressing *VAMP721* or *SYP121* with *RABA2a(Q71L)ΔC* but only very

211 weak signals in cells coexpressing the inactive mutant form *RABA2a(S26N)ΔC* (**Figure**
 212 **1H and 1I**). *RABA2a(Q71L)ΔC* failed to reconstitute YFP with VAMP723 or SYP123
 213 (**Figure 1H and 1I**), consistent with results from LCI and SU-Y2H assays. We also
 214 quantified the ratios of YFP/RFP fluorescence. We obtained no YFP signal and very
 215 low YFP/RFP ratios in cells coexpressing *cYFP* with *VAMP721* or *SYP121* and in cells
 216 coexpressing *RABA2a(Q71L)ΔC* with *VAMP723* or *SYP123* (**Figure 1H–1K**),
 217 suggesting that the interaction of RABA2a with VAMP721 or SYP121 is not non-
 218 specific. We also confirmed that the lack of YFP signal is not caused by lack of protein
 219 accumulation by immunoblot analysis (**Supplemental Figure 2K and 2L**).

220 Taken together, these results suggest that the SNARE proteins VAMP721 and
 221 SYP121 both function as the downstream effectors of RABA2a GTPase.

222

223 **VAMP721 and SYP121 selectively interact with some members of the RABA 224 family**

225 Since RABA2a belongs to the RABA family, which consists of six subclades, we
 226 investigated whether the interaction with VAMP721 and SYP121 was specific to
 227 RABA2a or shared by the other RABA homologs. We first showed that all the members
 228 from the RABA2 clade interacted with VAMP721 in SU-Y2H and LCI assays
 229 (**Supplemental Figure 4A and 4C**). However, only RABA2aΔC and RABA2cΔC
 230 showed interaction with SYP121 whereas only very weak interaction was detected
 231 between SYP121 and RABA2bΔC or RABA2dΔC in SU-Y2H and LCI assays
 232 (**Supplemental Figure 4B and 4D**). We next performed SU-Y2H experiments using
 233 RABA1bΔC, RABA3ΔC, RABA4bΔC, RABA5dΔC, and RABA6bΔC to represent the
 234 five remaining subclades. In addition to RABA2aΔC, RABA3ΔC also interacted with
 235 VAMP721, whereas RABA1bΔC, RABA4bΔC, RABA5dΔC, and RABA6bΔC did not
 236 (**Supplemental Figure 4E**). These results suggest that interaction with VAMP721 is
 237 not a common feature of all RABA GTPases but occurs only in some subclades of the
 238 RABA family. We also examined the interaction between VAMP721 and members of
 239 other clades in the RAB GTPase superfamily, including RABC2aΔC, RABD2bΔC,
 240 RABE1cΔC, RABF2bΔC, RABG3fΔC and RABH1bΔC, by SU-Y2H analysis. None

241 of the tested RAB GTPases showed significant interactions (**Supplemental Figure 4F**),
 242 further supporting the notion that the interaction between RABA2a and VAMP721 is
 243 not a universal phenomenon among all RAB GTPases but is unique to some members
 244 of the RABA family.

245

246 **RABA2a interacts with the entire members of the SNARE complex**

247 VAMP721/722, SYP121, and SOLUBLE N-ETHYLMALEIMIDE-SENSITIVE
 248 FACTOR ADAPTOR PROTEIN 33 (SNAP33) form the ternary SNARE complex and
 249 coordinately function in exocytosis in response to powdery mildew/oomycete infection
 250 (Kwon *et al.*, 2008). We performed SU-Y2H experiments to test whether RABA2a
 251 interacts with the other subunits of the SNARE complex. VAMP722 and SNAP33, like
 252 VAMP721, interacted with RABA2a Δ C and exhibited a stronger interaction with
 253 RABA2a(Q71L) Δ C but not with RABA2a(S26N) Δ C (**Supplemental Figure 5A and**
 254 **5B**). We validated this interaction by LCI, with strong luciferase activity for the
 255 combination of *RABA2a(Q71L) Δ C* with *VAMP722* or *SNAP33* but much weaker
 256 activity from cells coexpressing *RABA2a(S26N) Δ C* with *VAMP722* or *SNAP33*
 257 (**Supplemental Figure 5C and 5D**). These results indicate that RABA2a interacts with
 258 the entire members of the SNARE complex in its GTP-bound form.

259

260 **RABA2a affects the assembly of the SNARE complex**

261 Since RABA2a physically interacted with both VAMP721 and SYP121, we next
 262 examined the colocalization between the two sets of proteins by crossing
 263 *pRABA2a::YFP-RABA2a* with *pVAMP721::RFP-VAMP721* or *pUBQ10::RFP-SYP121*
 264 stable transgenic lines, hereafter referred to as YFP-RABA2a, RFP-VAMP721 and
 265 RFP-SYP121, respectively. Image analysis revealed that vesicles labeled by RFP-
 266 VAMP721 or RFP-SYP121 strongly correlate with YFP-RABA2a foci, with high
 267 Pearson's correlation coefficients (**Figure 2A and 2B**), suggesting that these proteins
 268 localize to the same subcellular compartments *in vivo*.

269 We then examined whether the interaction between RABA2a and
 270 VAMP721/722/SNAP33 might affect the assembly of the SNARE complex via a

271 transient *N. benthamiana* infiltration experiment. Consistent with published results, we
 272 detected strong YFP fluorescence when we coexpressed *VAMP721* with either *SYP121*
 273 or *SNAP33*, supporting the notion that the SNARE complex can be autonomously
 274 assembled in this transient infiltration system (**Figure 2C–2E**). Co-infiltration with
 275 *CFP-RABA2a* did not alter the intensity of YFP fluorescence in cells coexpressing
 276 *VAMP721* with *SYP121* or *SNAP33*, but overexpressing *CFP-RABA2a(Q71L)*
 277 enhanced YFP fluorescence intensity (**Figure 2D–2G**). By contrast, coexpressing *CFP-*
 278 *RABA2a(S26N)* markedly reduced the intensity of YFP fluorescence (**Figure 2D–2G**).
 279 These results suggest that RABA2a modulates the assembly of the SNARE complex
 280 depending on its GTP binding status. To further examine its specificity, we also checked
 281 the effects of RABA2a on another SNARE complex. VAMP711 interacts with SYP22
 282 and VESICLE TRANSPORT V-SNARE 11 (VTI11) to form a SNARE complex in the
 283 vacuolar sorting pathway (Fujiwara et al., 2014; Takemoto et al., 2018). We
 284 successfully reconstituted YFP when coexpressing the SNARE pair *nYFP-SYP22* and
 285 *cYFP-VAMP711* in a BiFC assay in transient *N. benthamiana* (**Supplemental Figure**
 286 **6A–6D**). However, coexpressing *RABA2a*, *RABA2a(Q71L)* or *RABA2a(S26N)* as a
 287 cyan fluorescent protein (CFP) fusion did not change the fluorescence intensity of the
 288 reconstituted YFP (**Supplemental Figure 6E–6G**). Collectively, these data suggest that
 289 RABA2a specifically regulates the VAMP721/722-SYP121-SNAP33 ternary complex.

290 We further tested the effects of RABA2a on the SNARE complex *in vivo* by co-IP
 291 analysis. Overexpressing *RABA2a(Q71L)* by β-estradiol induction did not significantly
 292 affect the interaction between VAMP721 and SYP121 (**Figure 2H and 2I**), probably
 293 because the interaction between the SNARE pair is already saturated in plants. However,
 294 overexpressing inactive *RABA2a(S26N)* markedly reduced the interaction between
 295 VAMP721 and SYP121 (**Figure 2J and 2K**), further confirming the notion that
 296 inactivated RABA2a disrupts the assembly of the SNARE complex *in vivo*.

297 Taken together, these findings indicate that RABA2a interacts with and modulates
 298 the assembly of the VAMP721/722-SYP121-SNAP33 SNARE ternary complex.
 299

300 **The exocyst subunits do not interact with RABA2a or the SNARE proteins**

301 Sec15 is the effector of the GTPase Rab11 in mammals (Zhang *et al.*, 2004). Active
 302 Rab11 interacts with Sec15 and subsequently recruits the entire exocyst prior to
 303 SNARE complex-mediated membrane fusion (Welz *et al.*, 2014; Wu *et al.*, 2005; Zhang
 304 *et al.*, 2004). In plants, genes encoding Rab11 homologs expanded during evolution
 305 (Rutherford and Moore, 2002). RABA2s are the closest paralogs of Rab11 based on
 306 sequence alignment (Rutherford and Moore, 2002). Therefore, we expected exocyst
 307 subunits to be strong candidates for RABA2a interaction based on results from yeast
 308 and mammals. However, we detected the exocyst subunits at much lower levels in the
 309 RABA2a interactome than expected, whereas the SNARE proteins showed much
 310 stronger interactions (**Supplemental Table 1**). This finding was unexpected, as classic
 311 cell biology studies suggest that the exocyst is required to anchor secretory vesicles to
 312 the PM prior to SNARE complex-mediated membrane fusion.

313 These IP-MS results prompted us to further explore the relationship of the exocyst
 314 with RABA2a and SNARE proteins via SU-Y2H. As a positive control,
 315 RABA2a(Q71L)ΔC interacted with VAMP721 and SYP121, supporting active growth
 316 of yeast (**Figure 3A and 3B**), similar to the results described above (**Figure 1B and**
 317 **1C**). By contrast, none of the exocyst subunits exhibited significant interaction with
 318 VAMP721 or SYP121 (**Figure 3A and 3B**). We also confirmed that the lack of
 319 interaction is not caused by a lack of protein accumulation (**Supplemental Figure 7A**
 320 and **7B**).

321 To further confirm the results, we next carried out LCI experiments. As a positive
 322 control, SYP121 showed strong interaction with both VAMP721 and
 323 RABA2a(Q71L)ΔC (**Figure 3C-3E**), similar to our previous results (**Supplemental**
 324 **Figure 3**); EXO84b strongly interacted with SEC15b (**Figure 3F**), similar to previous
 325 reports (Fendrych *et al.*, 2010; Hala *et al.*, 2008). By contrast, we detected no luciferase
 326 activity from the combination of VAMP721, SYP121 and RABA2a(Q71L)ΔC with
 327 SEC15b, EXO70A1 or EXO84b in the same *N. benthamiana* leaves (**Figure 3C-3F**),
 328 indicating that the exocyst subunits do not interact with RABA2a or the SNARE
 329 proteins.

330 We also examined the interaction between exocyst subunits and the other RAB

331 GTPases from RABA2 clade by LCI assays. As the positive control, all the RABA2
 332 GTPases showed strong interaction with VAMP721 (**Supplemental Figure 8A-8D**),
 333 consistent with the previous results (**Supplemental Figure 3A and 3B**), and EXO70A1
 334 strongly interacted with Patellin 3 (PATL3) (**Supplemental Figure 8E**), in accordance
 335 with the previous publication (Wu et al., 2017), indicating that the system worked as
 336 expected. However, we failed to detect luciferase activity in the combination of exocyst
 337 subunits and RABA2 GTPases in the same *N. benthamiana* leaves (**Supplemental**
 338 **Figure 8**).

339 We also performed a BiFC assay in *N. benthamiana*. As a positive control,
 340 VAMP721 interacted strongly with SYP121 and RABA2a(Q71L) Δ C (**Figure 3G and**
 341 **3H**), consistent with our previous results (**Figure 1H and Figure 2D**); and SEC15b
 342 strongly interacted with SEC10 (**Figure 3G and 3H**), similar to previous reports
 343 (Fendrych et al., 2010; Hala et al., 2008). By contrast, none of the exocyst subunits
 344 exhibited significant interaction with RABA2a(Q71L) Δ C or the downstream SNARE
 345 proteins (**Figure 3G and 3H**). We also confirmed that all proteins accumulated in the
 346 above-mentioned pairs by immunoblot analysis (**Supplemental Figure 7C-7F**).

347 We also validated these results *in vivo* via co-IP experiments. We used antibodies
 348 against SEC8 and SEC6, which have been reported before (Fendrych et al., 2010) and
 349 are commercially available. We also generated an antibody targeting SEC15b and
 350 verified its specificity (**Supplemental Figure 1C**). As a positive control, SEC8, SEC6,
 351 and SEC15b co-precipitated with EXO70A1-GFP and EXO84b-GFP, similar to
 352 previous findings (Fendrych et al., 2010; Hala et al., 2008). RABA2a co-precipitated
 353 with SYP121 and VAMP721 (**Figure 3I**), consistent with our other results (**Figure 1A**),
 354 implying that the system functioned as expected. By contrast, the exocyst subunits were
 355 absent in the co-precipitants with YFP-RABA2a, and SYP121 and VAMP721 were
 356 absent in the co-precipitants with the exocyst subunits (**Figure 3I**), further confirming
 357 the lack of interaction.

358 Together, these results support the notion that neither the GTPase RABA2a nor
 359 the downstream effector SNARE proteins interact with the exocyst complex, which is
 360 consistent with our MS analysis.

361

362 **RABA2a does not interact with SCD1**

363 The evolutionarily conserved Ypt31/32-Sec2p-Sec4p-exocyst pathway in yeast and
 364 the Rab11-Rabin8-Rab8-exocyst pathway in mammals form a GTPase activation
 365 cascade to coordinate vesicle transport with membrane tethering at the PM (Feng et al.,
 366 2012; He and Guo, 2009; Knodler *et al.*, 2010; Ortiz *et al.*, 2002; Sultana et al., 2011).
 367 In a comparable pathway in plants, the DENN domain-containing proteins SCD1 and
 368 SCD2 directly interact with both RABE1 GTPases and SEC15b (Mayers *et al.*, 2017).
 369 Since RABAs are paralogs of Rab11s and Ypt31/Ypt32 (Chow *et al.*, 2008), we
 370 reasoned that a parallel RABAs-SCD1/2-RABE1s-exocyst pathway might exist in
 371 plants. We further examined the interaction of RABA2a with SCD1 and RABE1s by
 372 co-IP. As a positive control, SCD1 co-precipitated with RABE1 and SEC15b (**Figure**
 373 **3J and 3K**), and RABE1d co-precipitated with the exocyst subunits SEC15b and SEC8
 374 (**Figure 3K**), consistent with previous results (Mayers *et al.*, 2017). However, RABA2a
 375 was absent from the co-precipitants with SCD1 or RABE1d (**Figure 3K**). These results
 376 suggest that RABA2a does not participate in the canonical RAB GTPase activation
 377 cascade. However, we cannot exclude the possibility that RABA subclade members
 378 other than RABA2a may participate in such a pathway.

379

380 **RABA2a does not affect the distribution or assembly of the exocyst complex**

381 Since RABA2a did not physically interact with the exocyst, we next investigated
 382 whether the RABA2a-mediated secretory pathway affected the distribution of the
 383 exocyst by first using endosidin 16 (ES16). ES16 was previously reported to
 384 preferentially interfere with the apical localized PIN2 but not the basal localized PIN1
 385 by disrupting the RABA2a-regulated secretory pathway (Li *et al.*, 2017b). We used the
 386 *PIN2-GFP* transgenic line as a positive control, based on a previous publication (Li *et*
 387 *al.*, 2017b). After treatment with 25 μM ES16 for 90 min, PIN2 aggregates clearly
 388 accumulated (**Supplemental Figure 9A**), consistent with the reduced signal ratio
 389 between the PM and cytoplasm (**Supplemental Figure 9B**). Similar to PIN2, SYP121
 390 and VAMP721 signals were also attenuated within the cells, and the signal ratio

391 between the PM and cytoplasm significantly reduced upon ES16 treatment
 392 (**Supplemental Figure 9A and 9B**). These results imply that the secretory route of
 393 SYP121 and VAMP721 is disrupted by ES16 treatment, which may be due to the
 394 inhibition of RABA2a activity. By contrast, ES16 did not alter the membrane
 395 distribution of EXO70A1 or EXO84b, and we detected no changes in their signal ratios
 396 between the PM and cytoplasm after ES16 treatment (**Supplemental Figure 9A and**
 397 **9B**).

398 To confirm these results, we carried out genetic experiments. Overexpressing the
 399 dominant negative *RABA2a(S26N)* by β-estradiol induction significantly reduced the
 400 PM localization of VAMP721 and SYP121 in root epidermal cells (**Figure 4A–4C, first**
 401 **and second row**). By contrast, we observed no significant changes in subcellular
 402 localization of the exocyst subunits EXO70A1 and EXO84b when overexpressing
 403 *RABA2A(S26N)* (**Figure 4A–4C, third and fourth row**). These genetic results support
 404 the notion that the RABA2a-mediated secretory pathway does not disturb the
 405 subcellular distribution of exocyst subunits.

406 We then investigated whether RABA2a regulates the assembly of the exocyst
 407 complex. Different exocyst subunits interact with each other to form a functional
 408 complex (Zarsky et al., 2013). However, overexpressing *RABA2a(Q71L)* or
 409 *RABA2a(S26N)* did not disrupt the interaction between the exocyst subunits, as all
 410 exocyst subunits properly immunoprecipitated with EXO84b in inducible lines
 411 compared to the non-induced control (**Figure 4D and 4E**), suggesting that RABA2a
 412 does not impair exocyst assembly. This result contrasts with the finding that
 413 overexpressing *RABA2a(S26N)* severely disturbed the assembly of the SNARE
 414 complex (**Figure 2J and 2K**). In summary, our findings demonstrate that the RABA2a-
 415 mediated secretory pathway does not affect the subcellular distribution or assembly of
 416 the exocyst.

417 As SCD1 and SCD2 are predicted to be the upstream regulators of the exocyst
 418 (Mayers et al., 2017), we also investigated the effects of RABA2a on SCD1. Neither
 419 ES16 treatment nor overexpressing *RABA2a(S26N)* had significant effects on the
 420 subcellular distribution of SCD1 (**Supplemental Figure 9C–9F**), suggesting that

421 RABA2a does not affect the upstream regulators of the exocyst complex. Taken
 422 together, our data suggest that RABA2a does not regulate the SCD1-exocyst pathway.
 423

424 **The exocyst does not interfere with the RABA2a-SNARE pathway**

425 Since RABA2a did not affect the subcellular localization or assembly of the
 426 exocyst, we examined mutual effects between the two pathways. We crossed *YFP-*
 427 *RABA2a*, *YFP-RABA2a(Q71L)*, *RFP-VAMP721*, and *GFP-SYP121* stable transgenic
 428 plants with heterozygous (+/-) plants for the exocyst subunit mutant *exo84b*. We used
 429 this mutant because loss of function in most other exocyst subunits leads to defects in
 430 pollen transmission (Bloch et al., 2016; Cole et al., 2005; Doucet et al., 2016; Li et al.,
 431 2013; Safavian et al., 2015; Synek et al., 2017), preventing us from obtaining
 432 homozygous null mutants for further analysis. EXO84b mutation was reported to
 433 disrupt the assembly of the exocyst complex, yet a null mutant with severe growth
 434 defects was viable (Synek et al., 2021). We determined the subcellular localization of
 435 RABA2a, RABA2a(Q71L), VAMP721, and SYP121 in homozygous *exo84b* plants in
 436 the F₃ generation. Although the *exo84b* null mutant exhibited severe growth defects
 437 (**Supplemental Figure 10**), the localization of RABA2a, RABA2a(Q71L), and
 438 SYP121 did not significantly change (**Figure 4F and 4G, first to third row**). However,
 439 the PM localization of VAMP721 was reduced in *exo84b*, along with increased
 440 intracellular signals (**Figure 4F and 4G, fourth row**), suggesting that the membrane
 441 localization of VAMP721 requires the proper functioning of both RABA2a and the
 442 exocyst complex. Although the localization of VAMP721 at the PM was reduced in the
 443 *exo84b* mutant, the colocalization between RABA2a and VAMP721 was enhanced
 444 rather than reduced in the mutant background compared to the control (**Figure 4H and**
 445 **4I**). The interaction of RABA2a with VAMP721 and SYP121 did not change in the
 446 *exo84b* mutant (**Figure 4J**). These results suggest that the *exo84b* mutant does not
 447 disrupt the RABA2a-SNARE association.

448 We also examined whether the *exo84b* mutant affected the assembly of the SNARE
 449 complex. We immunoprecipitated GFP-SYP121 in the *exo84b* mutant and examined
 450 the interaction between SYP121 and VAMP721 by immunoblot analysis. The EXO84b

451 mutation also did not alter the interaction between SYP121 and VAMP721 (**Figure 4K**),
 452 in contrast to the effect of *RABA2a(S26N)* overexpression, which severely disrupted the
 453 SYP121-VAMP721 interaction (**Figure 2J and 2K**). These results suggest that the
 454 exocyst subunit does not regulate the assembly of the SNARE complex, although the
 455 subcellular localization of VAMP721 requires proper function of the exocyst. Taken
 456 together, our data suggest that the exocyst does not interfere with the RABA2a-SNARE
 457 pathway.

458

459 **The exocyst and RABA2a-SNARE proteins follow different trafficking routes**
 460 **during the secretory process**

461 The above data suggest that the secretory pathways mediated by the exocyst and
 462 RABA2a-SNARE proteins are largely independent. We therefore examined the
 463 trafficking routes of the two pathways by spinning disk confocal (SDC) microscopy.
 464 Kymograph analyses revealed that VAMP721 foci co-migrated with the RABA2a foci
 465 at different time points but followed different trafficking routes from EXO84b and
 466 EXO70A1 foci (**Figure 5A–5I and Supplemental Movies 1–3**). We also analyzed the
 467 relationship between the three groups of vesicles by Z-stack imaging. VAMP721 foci
 468 colocalized with RABA2a foci in different Z sections from the top to middle section of
 469 cells. By contrast, we only detected EXO70A1 and EXO84b foci within top sections,
 470 and did not overlap with the VAMP721 foci (**Supplemental Figure 11A-C and**
 471 **Supplemental Movies 4–6**). In the surface area close to the PM, the colocalization
 472 coefficient between VAMP721 and EXO84b or EXO70A1 was also significantly
 473 lower than that between VAMP721 and RABA2a (**Figure 5J**). Furthermore, the
 474 vesicles labeled by EXO84b and EXO70A1 were much smaller than those labeled by
 475 RABA2a or VAMP721 (**Supplemental Movies 4–6 and Supplemental Figure 11D**).
 476 All these results indicate that VAMP721 and RABA2a foci represent a different type of
 477 vesicles from the membrane compartments targeted by the exocyst subunits. Such two
 478 types of vesicles follow different trafficking routes during the secretory process.

479

480 **The exocyst and RABA2a-SNARE pathways select different cargos in the**

481 **secretory pathways**

482 The above data suggest that the exocyst- and RABA2a-SNARE-mediated
 483 pathways function in parallel. Therefore, we analyzed whether the two pathways might
 484 select different cargos. RABA2a selectively regulates the recycling of PIN2, but not
 485 PIN1 (Li *et al.*, 2017b). The ABC transporter PENETRATION 3 (PEN3) requires the
 486 exocyst to recycle back to the PM (Mao *et al.*, 2016). We examined whether different
 487 PM proteins are differentially regulated through the exocyst and RABA2a-SNARE
 488 pathways. We crossed transgenic lines harboring *PIN2-GFP*, *PIN1-GFP*, or *PEN3-*
 489 *GFP* transgenes with plants heterozygous for the *exo84b* mutant or with the estradiol-
 490 inducible *RABA2a(S26N)* overexpression line. We then analyzed the subcellular
 491 localization and membrane distribution of the GFP-labeled proteins in homozygous F₃
 492 individuals. The membrane localization of PIN2 showed no obvious change in the
 493 *exo84b* mutant (**Figure 6A and 6B, first column**) but was mis-targeted to the
 494 intercellular vesicles in the inducible *RABA2a(S26N)* line (**Figure 6C-6E, first row**).
 495 By contrast, PEN3 relocated from the PM to the cytosol only in the *exo84b* mutant
 496 (**Figure 6A and 6B, third column**), but not in the *RABA2a(S26N)* overexpression line
 497 (**Figure 6C-6E, third row**). The subcellular distribution of PIN1 was not altered in
 498 either genotype (**Figure 6A and 6B, second column; Figure 6C-6E, second row**).
 499 These results indicate that the exocyst and RABA2a-SNARE secretory pathways select
 500 different cargos.

501

502 **The RABA2a-SNARE pathway is required for potassium homeostasis in plants**

503 We showed that the RABA2a-SNARE-mediated secretory pathway works largely
 504 independent of the exocyst. We next explored the physiological significance of this
 505 unique trafficking pathway. Both SYP121 and VAMP721 interact with the potassium
 506 (K⁺) channel POTASSIUM CHANNEL IN ARABIDOPSIS THALIANA 1 (KAT1)
 507 and are essential for the regulation of K⁺ uptake in plants (Grefen *et al.*, 2010a;
 508 Honsbein *et al.*, 2009; Zhang *et al.*, 2017). Therefore, we examined whether the
 509 RABA2a-SNARE-mediated secretory pathway also participates in this regulation by
 510 analyzing K⁺-dependent growth phenotypes. Alteration in K⁺ concentrations had

511 substantial effects on the growth of wild-type seedlings (**Figure 7A**), as reported
 512 previously (Li et al., 2017a). As the positive control, *syp121-1* single mutants were
 513 hypersensitive to lower K⁺ concentrations (**Supplemental Figure 12A and 12B**), as
 514 previously published (Honsbein *et al.*, 2009), indicating that our growth conditions are
 515 adequate to explore seedling responses to varying K⁺ supply. Overexpressing
 516 *RABA2a(S26N)* by β-estradiol induction had minor effects on main root growth under
 517 K⁺-sufficient conditions (19.26 ± 3.02 mm in wild type and 16.08 ± 3.43 mm in
 518 *RABA2a(S26N)* overexpression seedlings) (**Figure 7A–7C**). However, these seedlings
 519 exhibited a strong reduction in root elongation at lower K⁺ concentrations (**Figure 7A–**
 520 **7D**). Seedlings overexpressing *RABA2a(Q71L)* showed a wild-type-like response to
 521 reduced K⁺ supply (**Figure 7A–7D**). These data suggest that proper response to K⁺
 522 supply requires normal functions of RABA2a GTPase.

523 We next examined whether the exocyst subunits also participated in the regulation
 524 of K⁺ homeostasis. Since many exocyst subunit mutations cause severe male
 525 transmission defects or strong growth defects (Cole *et al.*, 2005; Fendrych *et al.*, 2010;
 526 Hala *et al.*, 2008; Zhang *et al.*, 2013), we cannot use the corresponding mutants for
 527 physiological experiments. Here, we chose *exo70b1-3* and *exo70b2-1*, which have been
 528 reported to be hypersensitive to powdery mildew infections but have no significant
 529 effects on growth pattern under normal conditions (Wang *et al.*, 2020; Zhao *et al.*, 2015).
 530 Both mutants showed similar response to K⁺ deficiency compared with the wild type
 531 control (**Supplemental Figure 12C and 12D**). We also did not observe a significant
 532 change in the response of *exo70f1* mutants under K⁺-deficient conditions, although the
 533 primary root length was slightly reduced under K⁺-sufficient conditions (17.71 ± 2.22
 534 mm in wild type and 15.44 ± 2.52 mm in *exo70f1*) (**Supplemental Figure 12E and**
 535 **12F**). We cannot choose *exo70a1* mutants due to sporophyte dysfunction and severe
 536 developmental defects (Synek *et al.*, 2006). They can only be propagated by
 537 heterozygous plants and therefore are not suitable for physiological experiments.

538 The above data indicate that RABA2a-SNARE regulated secretory pathway is
 539 important to maintain K⁺ homeostasis in plants.

541 **DISCUSSION**

542 In this study, we investigated the secretory pathway mediated by the TGN-localized
 543 small GTPase RABA2a. Through interactome analysis and further confirmation, we
 544 demonstrated that the SNARE proteins VAMP721 and SYP121 are the downstream
 545 effectors of RABA2a. We also explored the relationship between the RABA2a-
 546 SNARE- and SCD1-exocyst-mediated secretory pathways. Genetic, biochemical, and
 547 cell biology experiments suggested that the two pathways are largely independent,
 548 select different cargos and play different physiological roles. Our results suggest that a
 549 plant-specific RABA2a-SNARE pathway regulates the secretory process in parallel
 550 with the exocyst complex in plant cells. In the RABA2a-SNARE pathway, vesicles
 551 budding from the TGN bypass the tethering complex and fuse with the PM through
 552 interaction with the SNARE complex. PIN2, an auxin effluxer, is a cargo protein in this
 553 pathway. In parallel, exocyst-regulated exocytosis functions downstream of SCD1-
 554 RABE1 proteins. PEN3 is transported to the PM through this pathway. In addition, we
 555 showed that the RABA2a-SNARE-mediated secretory pathway fine-tunes K⁺
 556 homeostasis in plants. The results are summarized in the model shown in **Figure 7E**.

557 Compared to its yeast and mammalian counterparts, the plant TGN is a distinct
 558 organelle instead of simply a tubular reticulum on the trans side of the Golgi (Rosquete
 559 *et al.*, 2018). The plant TGN also functions as a sorting platform: it accepts Golgi-
 560 derived vesicles and also acts as an early endosome for recycling and further processing.
 561 To fulfill its function as a sorting hub, different RAB GTPases help organize the TGN
 562 into distinct subdomains. The functional diversification of the TGN subdomains in
 563 plant cells may explain the expansion of RABA families in the plant lineage (Jonsson
 564 *et al.*, 2017; Preuss *et al.*, 2004; Wattelet-Boyer *et al.*, 2016). In the current study, we
 565 characterized an unexpected RABA2a-SNARE interaction during the secretory process
 566 and demonstrated that the interaction is restricted to some members of the RABA2 and
 567 RABA3 subclades and does not occur with other RABA homologs or the other RAB
 568 GTPases. Our findings provide a deeper mechanistic understanding of TGN sub-
 569 compartmentalization and RABA GTPase-directed TGN sorting. We also demonstrated
 570 that the interaction between RABA2a and the SNARE proteins is restricted to some

571 members of the VAMP72 and SYP12 subclades, indicating that RABA2a-SNARE
572 interaction presents a unique sorting mechanism.

573 RAB and Rho GTPases function as the upstream signaling molecules for the
574 activation and recruitment of the exocyst to donor vesicles in yeast and mammalian
575 systems (Jin et al., 2011; Mukherjee et al., 2014; Ory and Gasman, 2011; Wu and Guo,
576 2015; Wu *et al.*, 2008). Following activation, the exocyst functions as a bridge that
577 connects incoming vesicles with the acceptor membrane synergistically with the
578 SNARE complex. For both systems, Sec15 interacts with Sec4 in yeast (Guo *et al.*,
579 1999) and with multiple RAB GTPases in mammalian cells, including RAB8, RAB11,
580 and RAB27, in a GTP-dependent manner (Feng *et al.*, 2012; Mei and Guo, 2018; Zhang
581 *et al.*, 2004). A comparable model based on published data has been proposed in yeast
582 and mammalian cells, whereby Ypt31/RAB11-Sec2/Rabin8-Sec4/RAB8-exocyst
583 interactions form a GTPase activation cascade that coordinates vesicle exit from the
584 donor membrane, with the latter tethered at the PM (Guo *et al.*, 1999; Welz *et al.*, 2014;
585 Wu *et al.*, 2005). Although all paralogs of the exocyst subunits in plants were identified
586 over a decade ago, few studies have explored the colocalization of exocyst subunits
587 with incoming vesicles or their direct interaction with the upstream RAB or ROP
588 GTPases. In the current study, we obtained multiple lines of evidence that RABA2a and
589 the downstream effector SNARE proteins do not interact with the exocyst subunits.
590 This observation is different from a recent publication that showed physical interaction
591 between exocyst subunits and VAMP721 and SYP121, and their synergistic functions
592 during secretory processes (Larson et al., 2020). In our work, the lack of interactions
593 between the exocyst subunits and RABA2a or SNARE proteins is supported by SU-
594 Y2H, LCI, BiFC and *in vivo* co-IP results. For each negative result, we present multiple
595 positive controls, including the interactions of VAMP721 with SYP121 or
596 RABA2a(Q71L) Δ C, and the interactions among exocyst subunits, which all agree with
597 previous reports (Fendrych *et al.*, 2010; Hala *et al.*, 2008). All the positive controls
598 supported the notion that our interaction assay conditions are adequate and are unlikely
599 to lead to spurious interactions. Our results were further supported by direct
600 visualization of the trafficking dynamics of the RABA2a-VAMP721 and exocyst-

601 VAMP721 pairs *in vivo* using SDC microscopy. Consistent with our cytological and
602 biochemical results, VAMP721 co-migrated with RABA2a but followed a distinct
603 trafficking route from the exocyst subunits. Furthermore, vesicles containing RABA2a
604 and VAMP721 were significantly larger than vesicles labeled by the exocyst subunits,
605 providing additional evidence that the two sets of vesicles form different populations
606 with distinct identities. This conclusion was further supported by our results
607 demonstrating that the two parallel pathways select different cargo proteins and play
608 different physiological roles. A recent publication by an independent group reported
609 that VAMP721 and VAMP722 play an important role in maintaining the morphology
610 of TGN and regulating TGN-derived secretory vesicles (Zhang et al., 2021). The PM
611 localization of PIN2 was severely disrupted in the *vamp721vamp722* double mutant
612 (Zhang et al., 2021). This is similar to seedlings overexpressing *RABA2a(S26N)*, but
613 very different from the *exo84b* mutant, in which PIN2 is still properly localized at the
614 PM. Their results, together with our data, strongly suggest that VAMP721 and
615 VAMP722 may act in the downstream of RABA2a to regulate the TGN-derived
616 secretory pathway. However, since different RABA paralogs and different isoforms of
617 the exocyst are present in plant systems, we cannot exclude the possibility that the other
618 RABA-SNARE pairs may function synergistically with the other exocyst isoforms.

619 SCD1 and SCD2 interact with SEC15b and RABE1 GTPases (Mayers et al., 2017).
620 Since SCD1 and SCD2 proteins contain a conserved DENN domain that is thought to
621 exhibit GEF activity, as shown for yeast Sec4 and mammalian Rabin8 proteins, one
622 might expect that a RABA-SCD1/SCD2-RABE-exocyst pathway may exist in plants,
623 as in yeast and mammalian cells. However, we failed to detect an interaction for
624 RABA2a GTPase with either RABE1 or SCD1 or the exocyst components in any assays,
625 suggesting that RABA2a does not participate in the canonical RAB activation cascade.
626 However, RABA GTPases other than RABA2a may fulfill these conserved functions.
627 Our genetic, biochemical, and cytological evidence also suggests that the RABA2a-
628 SNAREs and SCD1-exocyst pathways function in parallel in plants instead of along a
629 linear cascade, a hypothesis that is supported by their different levels of sensitivity to
630 ES16 treatment, as well as different cargo selections and different physiological roles.

631 Together, these data suggest that plants have generated different trafficking mechanisms
 632 in the secretory process.

633 Whereas two copies of *Ypt31/32* are present in yeast and three copies of *RAB11*
 634 genes exist in mammals, *RABA* paralogs expanded to 26 members in the model plant
 635 *Arabidopsis* (Rutherford and Moore, 2002; Vernoud *et al.*, 2003). Although all eight
 636 subunits of the exocyst have been identified in plants, most subunit genes are present
 637 with more than one copy, especially *Exo70* (Cvrckova *et al.*, 2012; Zhang *et al.*, 2010).
 638 Dozens of *Exo70* paralogs have been identified in each plant genome, many with
 639 diverse physiological functions, suggesting that different isoforms of the exocyst may
 640 exist in plant cells (Acheampong *et al.*, 2020; Brillada *et al.*, 2021; Pecenkova *et al.*,
 641 2011; Synek *et al.*, 2017). This fact may explain why we failed to detect the conserved
 642 RAB-exocyst-SNARE activation cascade in *Arabidopsis*, likely due to the selection
 643 specificity between different RABAs and different exocyst isoforms. Nonetheless, our
 644 findings support the notion that the RABA2a-mediated plant-specific secretory
 645 pathways can bypass the exocyst and that the two parallel pathways transport different
 646 cargos.

647 A recent publication indicates that the exocyst can be divided into two
 648 subcomplexes, which are recruited to PM through the interaction of EXO70A1 with
 649 phosphoinositides (Synek *et al.*, 2021). In yeast, it has been reported that
 650 phosphoinositides can activate SNARE chaperones for the recruitment of R-SNARE
 651 into fusion-competent SANRE complexes and promote synergistic SNARE complex
 652 remodeling for membrane fusion (Mima and Wickner, 2009). Future work will further
 653 explore the relationship between exocyst subunits, SNARE proteins, and
 654 phosphoinositides. Studies in yeast also indicate that some exocyst subunits directly
 655 interact with the SNARE regulator Sec1/Munc18 (SM) proteins (Morgera *et al.*, 2012).
 656 Since we did not detect the direct interaction between exocyst subunits and SNARE
 657 proteins, we can expect that SM proteins may serve as the bridge to link the function
 658 between exocyst and SNARE complex in plants although this hypothesis requires
 659 further support from experimental data.

660 In summary, our findings shed light on a unique trafficking mechanism in plant

661 cells. The plant endomembrane system has developed many unique properties via the
 662 expansion of gene families and the functional differentiation or evolution of novel
 663 functions for the encoded proteins. Our study of RABA2a and the exocyst complex
 664 provides a good example of how highly conserved endomembrane proteins develop
 665 plant-specific trafficking mechanisms. Future work will focus on further exploring the
 666 physiological significance of the two parallel secretory pathways.

667

668 METHODS

669 Plant Materials and Growth Conditions

670 *Arabidopsis thaliana* accession Columbia 0 (Col-0) was used as the wild type (WT) in
 671 this study. Stable transgenic lines harboring the following transgenes were described
 672 previously: *PIN1-GFP* (Friml et al., 2002), *PIN2-GFP* (Xu and Scheres, 2005), *GFP-*
 673 *SYP121* (Collins et al., 2003), *PEN3-GFP* (Stein et al., 2006), *RFP-VAMP721*
 674 (Ichikawa et al., 2014), *YFP-RABA2a* (Chow et al., 2008), *SEC6-GFP* (Fendrych et al.,
 675 2010), *SEC8-GFP* (Fendrych et al., 2010), *EXO70A1-GFP* (Fendrych et al., 2010),
 676 *EXO84b-GFP* (Fendrych et al., 2010), *SCD1-GFP* (Mayers et al., 2017),
 677 *pUBQ10::YFP* (Geldner et al., 2009), *YFP-RABC1* (Geldner et al., 2009), *YFP-*
 678 *RABD2a* (Geldner et al., 2009) and *YFP-RABE1d* (Geldner et al., 2009). The T-DNA
 679 insertion lines *exo84b* (GK-459C01), *vamp721* (SALK_037273C), and *vamp722*
 680 (SALK_103189C) and *exo70f1* (SALK_139110) were obtained from the Arabidopsis
 681 Biological Resource Center (ABRC). The T-DNA insertion mutants *exo70b1-3* and
 682 *exo70b2-1*(SALK_091877C) were described previously (Zhao et al., 2015). The
 683 marker lines were introduced into the *exo84b* homozygous mutant by crossing, and
 684 marker lines in the *exo84b* (+/-) heterozygous mutant background were identified by
 685 genotyping.

686 Seeds were surface sterilized in 0.25% sodium hypochlorite, washed four times
 687 with sterile water, and allowed to hydrate at 4°C for 2 days in the dark. For confocal
 688 observation or protein extraction, seeds were sown on half-strength Murashige & Skoog
 689 (MS, PhytoTech, M524) medium (pH 5.6) with 1% (w/v) sucrose and 0.8% (w/v) agar.
 690 For K⁺ dependent growth assays, seeds were sown on MS medium (Coolaber, PM1011)

691 or MS medium lacking K⁺ (MS-K, Coolaber, PM1011-K) (pH 5.6) with 1% (w/v)
 692 sucrose and 0.8% (w/v) agar. Plates were placed vertically in a growth chamber
 693 (Percival CU-36L) at 22°C under a long-day photoperiod (16 h light/8 h dark) for the
 694 indicated time.

695

696 **Vector Construction and *Arabidopsis* Transformation**

697 To generate the destination vectors pMDC7-GFP-Dest and pMDC7-RFP-Dest, the full-
 698 length *GFP* or *RFP* sequence without the stop codon was cloned into the pMDC7 vector
 699 digested with XhoI and ligated using a Seamless Cloning and Assembly kit (TransGen
 700 Bio, Beijing). Subsequently, the coding sequences of *RABA2a* or its mutated versions
 701 were amplified from plasmids and introduced into pDONR207, followed by LR
 702 recombination (Gateway LR clonase mix, Thermo Fisher) into pMDC7-GFP-Dest or
 703 pMDC7-RFP-Dest. To generate the *pUBQ10::RFP-SYP121* construct, the coding
 704 sequence of *SYP121* was amplified from cDNA and introduced into pDONR207,
 705 followed by the destination vector *pUBQ10::RFP-DEST* (Grefen et al., 2010b). Primer
 706 sequences are listed in Supplemental Table 2. All constructs were introduced into
 707 *Arabidopsis* accession Col-0 via Agrobacterium (*Agrobacterium tumefaciens*, strain
 708 GV3101)-mediated transformation using the floral-dip method (Clough and Bent,
 709 1998).

710

711 **SU-Y2H Assays**

712 To test protein-protein interactions in the SU-Y2H system, the coding sequences of
 713 *VAMP721*, *VAMP722*, *VAMP723*, *VAMP726*, *VAMP727*, *SYP121*, *SYP122*, *SYP123*,
 714 *SYP124*, *SYP125* and *SNAP33* were amplified from plasmids or cDNA and ligated into
 715 the pBT3-N bait vector with T4 ligase (Invitrogen, EL0011); the coding sequences of
 716 *SEC15b*, *EXO70A1*, *EXO84b*, *RABA1bΔC*, *RABA2aΔC*, *RABA2a(Q71L)ΔC*,
 717 *RABA2a(S26N)ΔC*, *RABA2bΔC*, *RABA2cΔC*, *RABA2dΔC*, *RABA3ΔC*, *RABA4bΔC*,
 718 *RABA5dΔC*, *RABA6bΔC*, *RABC2aΔC*, *RABD2bΔC*, *RABE1cΔC*, *RABF2bΔC*, and
 719 *RABH1bΔC* were ligated into the pPR3N prey vector. The expression of *EXO70A1*,
 720 *EXO84b*, and *RABA2a(Q71L)ΔC* induced strong self-activation when introduced into

721 the bait vectors. SU-Y2H assays were performed as previously described (Estevez,
 722 2015). Yeast strain NMY51 was co-transformed with pairs of pBT3-N bait and pPR3N
 723 prey vectors. The pOstI-NubI and pPR3N-NubG vectors were used as the positive and
 724 negative control, respectively.

725

726 LCI Assays

727 The Original vectors of pCAMBIA1300-35SN-cLUC and pCAMBIA1300-35SC-
 728 nLUC were reported previously (Chen et al., 2008). To generate pCAMBIA1300-
 729 35SN-nLUC vector, pCAMBIA1300-35SN-cLUC vector was double-digested with
 730 restriction enzymes SacI and SalI and ligated with SacI- and SalI-digested nLUC
 731 fragment with T4 ligase. Next, the pCAMBIA1300-35SN-cLUC were digested with
 732 KpnI and SalI and the pCAMBIA1300-35SN-nLUC was digested with SalI and
 733 purified for in-fusion cloning. The generated constructs of *cLUC-RABA2aΔC*, *cLUC-*
 734 *RABA2a(Q71L)ΔC*, *cLUC-RABA2a(S26N)ΔC*, *cLUC-RABA2bΔC*, *cLUC-RABA2cΔC*,
 735 *cLUC-RABA2dΔC*, *cLUC-VAMP721*, *cLUC-SYP121*, *cLUC-PATL3*, *cLUC-SEC15b*,
 736 *nLUC-VAMP721*, *nLUC-VAMP722*, *nLUC-VAMP723*, *nLUC-VAMP726*, *nLUC-*
 737 *SYP121*, *nLUC-SYP122*, *nLUC-SYP123*, *nLUC-SYP124*, *nLUC-SYP125*, *nLUC-*
 738 *SNAP33*, *nLUC-SEC15b*, *nLUC-EXO70A1*, and *nLUC-EXO84b* were transformed into
 739 Agrobacterium strain GV3101. *Nicotiana benthamiana* plants were grown at 26°C in a
 740 phytotron under a long-day photoperiod (16 h light/8 h dark). Four-week-old plants
 741 were used for agroinfiltration. The LCI assay was performed as described previously
 742 (Chen et al., 2008). Agrobacterium colonies were grown overnight to a final OD₆₀₀ of
 743 1–2. The cultures were pelleted by centrifugation and resuspended in infiltration buffer
 744 (10 mM MgCl₂, 10 mM 2-(*N*-morpholino)-ethanesulfonic acid (MES), pH 5.5, 150 μM
 745 acetosyringone), adjusted to OD₆₀₀ = 0.05. The p19 silencing suppressor was used to
 746 enhance protein expression and the cell suspension was adjusted to OD₆₀₀ = 0.1 in
 747 infiltration buffer. Pairs of agrobacteria carrying *nLUC* and *cLUC* constructs and the
 748 p19 suppressor were infiltrated into different locations of the same *N. benthamiana*
 749 leaves. The plants were allowed to recover for 2 days at 26°C and LCI images were
 750 captured by a low-light, cooled, charge-coupled device imaging apparatus (Tanon-5200,

751 Shanghai).

752

753 **BiFC Assays**

754 To test protein-protein interactions with the 2in1 BiFC cloning system, the coding
755 sequences of interest were amplified by PCR and cloned into the pDONR221-P3P2 or
756 pDONR221-P1P4 entry vectors. The resulting entry vectors were recombined into the
757 destination vector *pBiFCt-2in1-NN* (Grefen and Blatt, 2012) via LR reaction. All
758 constructs were transformed into Agrobacterium strain GV3101 and infiltrated into *N.*
759 *benthamiana* leaves as described above. The plants were allowed to recover for 2 days
760 at 26°C, and confocal images were captured with a Leica SP8 microscope.

761

762 **Co-IP Assays**

763 Co-IP was carried out as previously described (Heard et al., 2015) with minor
764 modifications. Seven-day-old seedlings were soaked in crosslinking buffer (Phosphate
765 Buffered Saline [PBS], pH 7.4, and 1 mM dithiobis [Invitrogen, 22585]) for 1 h at room
766 temperature. The reaction was terminated by the addition of 20 mM Tris-HCl, pH 7.5,
767 and incubation for 30 min. The samples were ground in a prechilled mortar and pestle
768 on ice with extraction buffer (150 mM Na-HEPES, pH 7.5, 10 mM EDTA, 10 mM
769 EGTA, 17.5% [w/v] sucrose, 7.5 mM KCl, 0.01% [v/v] Igepal CA-630, 10 mM
770 dithiothreitol, 1% [v/v] protease inhibitors [Sigma], 0.5% [v/v] polyvinylpolypyrrolidone),
771 with 2 mL buffer per 1 g of tissue (fresh weight). The homogenate was filtered through two layers of Miracloth (475855-1R, Millipore), and
772 the flow-through was centrifuged at 4°C, 6,000 g for 15 min. For the co-IP assay, 20 µL
773 GFP-Trap Sepharose beads (gta-20, ChromoTek) was added to the supernatant,
774 followed by incubation for 6 h at 4°C. The slurry was washed five times with prechilled
775 extraction buffer (no polyvinylpolypyrrolidone or protease inhibitors). The slurry was
776 collected after the last wash and proteins eluted with 5× SDS-PAGE loading buffer for
777 liquid chromatography-tandem MS (LC-MS/MS) or immunoblot analysis. The LC-
778 MS/MS assay was conducted by Protein World Biotech Ltd. (Beijing).

780

781 **Antibodies and Immunoblot Analysis**

782 To generate the anti-VAMP721, anti-SYP121, and anti-SEC15b antibodies, fragments
 783 of coding sequences encoding amino acids (aa) 1–193 of VAMP721, aa 1–284 of
 784 SYP121, and aa 50–272 of SEC15b were separately subcloned into the pGEX-4T-1
 785 vector (GE Healthcare). The resulting constructs carrying *VAMP721* and *SYP121* were
 786 sent to HUABIO Biotechnology Company (Hangzhou, China) for immunization and
 787 antibody purification, whereas the SEC15b antibody was produced at ABclonal
 788 Company (Wuhan, China). For each antibody, two rabbits were immunized. The
 789 antibodies were affinity-purified using HiTrap Columns coupled with antigens.

790 To confirm construct expression in SU-Y2H assay, yeast cells were harvested from
 791 6 mL selective medium after growth for 2 days by centrifugation at 5,000 g, and protein
 792 extraction was performed as reported recently (Emily R Larson, 2020). Prepared protein
 793 samples were loaded on 10% polyacrylamide gels and blotted onto a nitrocellulose
 794 membrane. Protein gel blotting was performed using the following antibodies: anti-HA
 795 (1:5,000, Sigma-Aldrich, H9658), anti-VAMP721 (1:1,000, HUABIO), anti-
 796 SYP121(1:1,000, HUABIO) or anti-VP16 (1:1,000, Abcam, ab4808).

797 To confirm protein accumulation from infiltrated BiFC constructs, *N.
 798 benthamiana* leaves were ground in a prechilled mortar and pestle on ice with extraction
 799 buffer as described in the co-IP assay. The isolated supernatants were electrophoresed
 800 on 10% SDS-PAGE and blotted onto a nitrocellulose membrane. Protein gel blotting
 801 was performed using the following antibodies: anti-HA (1:5,000, Sigma-Aldrich,
 802 H9658), anti-MYC (1:5,000, Sigma-Aldrich, SAB2702192), anti-RFP (1:1,000,
 803 Chromotek, 5F8).

804 The co-IP samples were run on 10% (w/v) SDS-PAGE gels and electroblotted onto
 805 nitrocellulose filter membranes. Protein gel blotting was performed using the following
 806 antibodies: anti-GFP (1:5,000; Sigma-Aldrich, SAB2702197), anti-RFP (1:1,000;
 807 Chromotek, 5F8), anti-RABA2a (1:1,000; PhytoAB, PHY0833S), anti-SEC6 (1:1,000;
 808 Agrisera, AS132686), anti-SEC8 (1:1,000; Agrisera, AS132708), anti-RABE1 (1:5,000,
 809 raised in chicken) (Speth et al., 2009), anti-SYP121 (1:1,000; HUABIO), anti-
 810 VAMP721 (1:1,000; HUABIO), and anti-SEC15b (1:1,000; ABclonal). The following

secondary antibodies were used: mouse antibody conjugated to HRP (1:10,000; Sangon; D110087), rabbit antibody conjugated to HRP (1:10,000; Sangon, D110058), chicken antibody conjugated to HRP (1:10,000; Abbkine, A21080), and anti-rat antibody conjugated to HRP (1:1,000 dilution; Sino Biological, SSA005).

815

816 **Chemical Treatments**

Stock solutions (1,000×) of 25 mM ES16 (Cambridge ID 5470964) (Li *et al.*, 2017b) and 5 mM β-estradiol (Sigma-Aldrich, E8875) were dissolved in DMSO, and 4 mM FM4-64 (Invitrogen, F34653) was dissolved in deionized water. ES16 was aliquoted for one-time use to eliminate freeze-thaw cycles. Treatments were performed as described previously (Li *et al.*, 2017b).

822

823 **Confocal Microscopy and Quantitative Analysis of Images**

All confocal images were captured on a Leica SP8 microscope. CFP signals were excited at 448nm and emission was detected at 460–500 nm. GFP signals were excited at 488nm and emission was detected at 505–545 nm. YFP were excited at 514 nm and emission was detected at 520–545nm. RFP were excited at 552 nm and emission was detected at 570–620 nm. FM4-64 were excited at 552 nm and emission was detected at 570–620 nm. Colocalization was determined using ImageJ software (<https://imagej.net/Fiji.html>) with the PSC colocalization plug-in (<http://www.c�ib.ac.uk/~afrench/coloc.html>) (French *et al.*, 2008). To analyze the ratio of signals at the PM/cytoplasm, fluorescence from F₃ progeny was captured and the ratios calculated using Image J software. To quantify the YFP/RFP ratio, entire images of the YFP or RFP channels were selected, the mean intensity recorded with Image J software, and the YFP/RFP ratio calculated. The signal intensity between the PM and cytoplasm was quantified by creating a region of interest encompassing the entire cytoplasm or entire PM domain. The mean intensity was recorded with ImageJ software and the ratio calculated.

839

840 **SDC Microscopy and Image Quantification**

841 SDC imaging was performed on a Nikon Ti2-E inverted microscope equipped with a
 842 Yokogawa CSU-W1 spinning disc unit and a Plan-Apo 100× objective (NA1.49). GFP
 843 and RFP were excited by laser at 488 nm/45 mW (Virtran) and 561 nm/100 mW
 844 (Coherent), respectively, and collected at 505–545 nm and 589–625 nm, respectively.
 845 Time-lapse and Z-stack images were recorded by an Orca-Fusion sCMOS camera in 3-
 846 s time intervals or 0.4-μm step size, respectively. The cell surface panels of GFP and
 847 RFP channels were extracted and further subjected to Pearson Correlation Coefficient
 848 analysis after background subtraction, through the image J plugin ‘Coloc2’ using
 849 default parameters. Kymograph analysis was performed as described previously (Zhang
 850 et al., 2019). Vesicle diameter was calculated using Imaris software (version 9.0.1,
 851 Bitplane) as described previously (Zhang et al., 2020).

852

853 **Accession Numbers**

854 Sequence data in this article can be found in the Arabidopsis Genome Initiative or
 855 GenBank/EMBL databases under the following accession numbers: *RABA1b*
 856 (At1g16920), *RABA2a* (At1g09630), *RABA2b* (At1g07410), *RABA2c* (At3g46830),
 857 *RABA2d* (At5g59150), *RABA3* (At1g01200), *RABA4b* (At4g39990), *RBA45d*
 858 (At2g31680), *RABA6b* (At1g18200), *RABC1* (At1g43890), *RABC2a* (At5g03530),
 859 *RABD2b* (At5g47200), *RABE1c* (At3g46060), *RABF2b* (At4g19640), *RABG3f*
 860 (At3g18820), *RABH1b* (At2g44610), *VAMP721* (At1g04750), *VAMP722* (At2g33120),
 861 *VAMP723* (At2g33110), *VAMP726* (At1g07460), *VAMP727* (At3g54300), *SYP121*
 862 (At3g11820), *SYP122* (At3g52400), *SYP123* (At4g03330), *SYP124* (At1g61290),
 863 *SYP125* (At1g11250), *SNAP33* (At5g61210), *SEC6* (At1g71820), *SEC8* (At3g10380),
 864 *SEC10* (At5g12370), *SEC15b* (At4g02350), *EXO70A1* (At5g03540), *EXO84b*
 865 (At5g49830), *PATL3* (At1g72160), *SCDI* (At1g49040), *PIN1* (At1g73590), *PIN2*
 866 (At5g57090) and *PEN3* (At1g59870),

867

868 **AUTHOR CONTRIBUTIONS**

869 RX.L. supervised the work. L.P. and RX.L. designed most of the experiments. Y.M. and
 870 RL.L. also contributed to the experimental design. L.P. performed most of the

871 experiments and analyzed the data.. Z.M. carried out the SDC imaging and kymograph
872 analysis. X.Z. quantified the size of vesicles. Y.H. helped with the construction of
873 vectors. L.P. and RX.L. wrote the manuscript. All authors agreed with the final
874 manuscript and its submission for publication.

875

876 **ACKNOWLEDGEMENTS**

877 We thank Prof. Christopher Grefen (University of Tübingen) for kindly providing the
878 pBiFCt-2in1 cloning vectors, the *pUBQ10::RFP-DEST* vector and the *pUBQ10::CFP-*
879 *DEST* vector, Prof. Xing Wang Deng (Peking University) for the LCI vectors, Prof. Li-
880 Jia Qu (Peking University) for the SU-Y2H vectors, and Prof. Shauna Somerville
881 (University of California, Berkeley) for the *PEN3-GFP* transgenic line, and Prof. Yun
882 Xiang (Lanzhou University) for the seeds of *exo70fl* mutant, and Prof. Dingzhong Tang
883 (Fujian Agriculture and Forestry University) for the seeds of *exo70b1-3* and *exo70b2-*
884 *I* mutants. This work was supported by the Key Laboratory of Molecular Design for
885 Plant Cell Factory of Guangdong Higher Education Institutes (2019KSYS006) and was
886 also financially supported by grants from the Natural Science Foundation of China
887 (31770306), Natural Science Foundation of Guangdong Province (2020A1515010966),
888 Guangdong Innovation Research Team Fund (2016ZT06S172), and the Shenzhen Sci-
889 Tech Fund (KYTDPT20181011104005). Z.M. and Y. M were supported financially by
890 Singapore Ministry of Education (MOE) Tier 1 (RG32/20) and Tier 3 (MOE2019-T3-
891 1-012). X.Z. was supported financially by National Science Foundation for Young
892 Scientists of China (32000558) and China Postdoctoral Science Foundation Grant
893 (2019M660494). RL.L. was supported financially by Natural Science Foundation of
894 China (31970182, 31670182) and the Fundamental Research Funds for the Central
895 Universities (2019ZY29).

896

897 **COMPETING INTERESTS**

898 The authors declare no competing interests.

899

900

901

902

903 **Supplemental Figures**904 **Supplemental Figure 1.** Characterization of the antibodies against SYP121,
905 VAMP721, and SEC15b.906 **Supplemental Figure 2.** Protein accumulation levels in split-ubiquitin yeast two-
907 hybrid (SU-Y2H) assays and bimolecular fluorescence complementation (BiFC)
908 assays corresponding to Figure 1.909 **Supplemental Figure 3.** Detection of protein interactions by luciferase
910 complementation imaging (LCI) assays.911 **Supplemental Figure 4.** VAMP721 and SYP121 selectively interact with some
912 members of the RABA family.913 **Supplemental Figure 5.** RABA2a interacts with the entire SNARE complex.914 **Supplemental Figure 6.** RABA2a does not affect the assembly of the SNARE
915 complex in the vacuolar sorting pathway.916 **Supplemental Figure 7.** Protein accumulation levels in split-ubiquitin yeast two-
917 hybrid (SU-Y2H) assays and bimolecular fluorescence complementation (BiFC)
918 assays corresponding to Figure 3.919 **Supplemental Figure 8.** The exocyst subunits do not interact with all the members
920 from RABA2 clade.921 **Supplemental Figure 9.** ES16 treatment and *RABA2a(S26N)* overexpression do not
922 affect the subcellular localization of exocyst subunits and SCD1.923 **Supplemental Figure 10.** Growth defects of the *exo84b* mutant.924 **Supplemental Figure 11.** Co-localization analysis by Z-series scan by spinning disc
925 confocal (SDC) microscopy.926 **Supplemental Figure 12.** The *exo70s* mutants show normal response to K⁺
927 deficiency.

928

929 **Supplemental Tables**930 **Supplemental Table 1.** Liquid chromatography-tandem mass spectrometry (LC-

931 MS/MS) data for the analysis of RABA2a GTPase interactors.

932 **Supplemental Table 2.** Primers used in this study.

933

934 **Supplemental Movies**

935 **Supplemental Movie 1.** RABA2a foci (green) co-migrate with VAMP721 foci
936 (magenta). Images were taken every 3 s.

937 **Supplemental Movie 2.** EXO84b foci (green) show distinct trafficking routes from
938 VAMP721 foci (magenta). Images were taken every 3 s.

939 **Supplemental Movie 3.** EXO70A1 foci (green) show distinct trafficking routes from
940 VAMP721 foci (magenta). Images were taken every 3 s.

941 **Supplemental Movie 4.** Z-series shows that VAMP721 foci (magenta) colocalize
942 with RABA2a foci (green) from top to middle sections. Images were taken by 0.4
943 $\mu\text{m}/\text{step}$.

944 **Supplemental Movie 5.** Z-series shows that VAMP721 foci (magenta) do not
945 colocalize with EXO84b foci (green) from top to middle sections. Images were taken
946 by 0.4 $\mu\text{m}/\text{step}$.

947 **Supplemental Movie 6.** Z-series shows that VAMP721 foci (magenta) do not
948 colocalize with EXO70A1 foci (green) from top to middle sections. Images were
949 taken by 0.4 $\mu\text{m}/\text{step}$.

950

951 **REFERENCES**

952 **Acheampong, A.K., Shanks, C., Cheng, C.Y., Schaller, G.E., Dagdas, Y., and**
953 **Kieber, J.J.** (2020). EXO70D isoforms mediate selective autophagic degradation of
954 type-A ARR proteins to regulate cytokinin sensitivity. Proc Natl Acad Sci U S A
955 **117**:27034-27043. 10.1073/pnas.2013161117.

956 **Antignani, V., Klocko, A.L., Bak, G., Chandrasekaran, S.D., Dunivin, T., and**
957 **Nielsen, E.** (2015). Correction. Plant Cell **27**:2664-2665. 10.1105/tpc.15.00761.

958 **Berson, T., von Wangenheim, D., Takac, T., Samajova, O., Rosero, A., Ovecka,**
959 **M., Komis, G., Stelzer, E.H., and Samaj, J.** (2014). Trans-Golgi network localized

- 960 small GTPase RabA1d is involved in cell plate formation and oscillatory root hair
 961 growth. *Bmc Plant Biol* **14**:252. 10.1186/s12870-014-0252-0.
- 962 **Bloch, D., Pleskot, R., Pejchar, P., Potocky, M., Trpkosova, P., Cwiklik, L.,**
 963 **Vukasinovic, N., Sternberg, H., Yalovsky, S., and Zarsky, V.** (2016). Exocyst SEC3
 964 and Phosphoinositides Define Sites of Exocytosis in Pollen Tube Initiation and
 965 Growth. *Plant Physiol* **172**:980-1002. 10.1104/pp.16.00690.
- 966 **Brillada, C., Teh, O.K., Ditengou, F.A., Lee, C.W., Klecker, T., Saeed, B., Furlan,**
 967 **G., Zietz, M., Hause, G., Eschen-Lippold, L., et al.** (2021). Exocyst subunit
 968 Exo70B2 is linked to immune signaling and autophagy. *Plant Cell* **33**:404-419.
 969 10.1093/plcell/koaa022.
- 970 **Chen, H., Zou, Y., Shang, Y., Lin, H., Wang, Y., Cai, R., Tang, X., and Zhou, J.M.**
 971 (2008). Firefly luciferase complementation imaging assay for protein-protein
 972 interactions in plants. *Plant Physiol* **146**:368-376. 10.1104/pp.107.111740.
- 973 **Choi, S.W., Tamaki, T., Ebine, K., Uemura, T., Ueda, T., and Nakano, A.** (2013).
 974 RABA members act in distinct steps of subcellular trafficking of the FLAGELLIN
 975 SENSING2 receptor. *Plant Cell* **25**:1174-1187. 10.1105/tpc.112.108803.
- 976 **Chong, Y.T., Gidda, S.K., Sanford, C., Parkinson, J., Mullen, R.T., and Goring,**
 977 **D.R.** (2010). Characterization of the *Arabidopsis thaliana* exocyst complex gene
 978 families by phylogenetic, expression profiling, and subcellular localization studies.
 979 *New Phytol* **185**:401-419. 10.1111/j.1469-8137.2009.03070.x.
- 980 **Chow, C.M., Neto, H., Foucart, C., and Moore, I.** (2008). Rab-A2 and Rab-A3
 981 GTPases define a trans-golgi endosomal membrane domain in *Arabidopsis* that
 982 contributes substantially to the cell plate. *Plant Cell* **20**:101-123.
 983 10.1105/tpc.107.052001.
- 984 **Clough, S.J., and Bent, A.F.** (1998). Floral dip: a simplified method for
 985 Agrobacterium-mediated transformation of *Arabidopsis thaliana*. *Plant J* **16**:735-743.

- 986 10.1046/j.1365-313x.1998.00343.x.
- 987 **Cole, R.A., Synek, L., Zarsky, V., and Fowler, J.E.** (2005). SEC8, a subunit of the
988 putative *Arabidopsis* exocyst complex, facilitates pollen germination and competitive
989 pollen tube growth. *Plant Physiol* **138**:2005-2018. 10.1104/pp.105.062273.
- 990 **Collins, N.C., Thordal-Christensen, H., Lipka, V., Bau, S., Kombrink, E., Qiu,
991 J.L., Huckelhoven, R., Stein, M., Freialdenhoven, A., Somerville, S.C., et al.**
992 (2003). SNARE-protein-mediated disease resistance at the plant cell wall. *Nature*
993 **425**:973-977. 10.1038/nature02076.
- 994 **Cvrckova, F., Grunt, M., Bezvoda, R., Hala, M., Kulich, I., Rawat, A., and
995 Zarsky, V.** (2012). Evolution of the land plant exocyst complexes. *Front Plant Sci*
996 **3**:159. 10.3389/fpls.2012.00159.
- 997 **Das, A., and Guo, W.** (2011). Rabs and the exocyst in ciliogenesis, tubulogenesis and
998 beyond. *Trends Cell Biol* **21**:383-386. 10.1016/j.tcb.2011.03.006.
- 999 **Ding, Y., Robinson, D.G., and Jiang, L.** (2014). Unconventional protein secretion
1000 (UPS) pathways in plants. *Curr Opin Cell Biol* **29**:107-115.
1001 10.1016/j.ceb.2014.05.008.
- 1002 **Doucet, J., Lee, H.K., and Goring, D.R.** (2016). Pollen Acceptance or Rejection: A
1003 Tale of Two Pathways. *Trends Plant Sci* **21**:1058-1067. 10.1016/j.tplants.2016.09.004.
- 1004 **Emily R Larson, J.O., Naomi Alice Donald, Jonas Chaves Alvim, Mike R. Blatt
1005 and Viktor Zarsky** (2020). Synergy Among Exocyst and SNARE Interactions
1006 Identifies a Functional Hierarchy in Secretion during Vegetative Growth. DOI
1007 10.1105/tpc.20.00280.
- 1008 **Estevez, J.M.** (2015). Plant Cell Expansion. *Methods and Protocols* 10.1007/978-1-
1009 4939-1902-4_13.
- 1010 **Fendrych, M., Synek, L., Pecenkova, T., Drdova, E.J., Sekeres, J., de Rycke, R.,**

- 1011 **Nowack, M.K., and Zarsky, V.** (2013). Visualization of the exocyst complex
 1012 dynamics at the plasma membrane of *Arabidopsis thaliana*. *Mol Biol Cell* **24**:510-520.
 1013 10.1091/mbc.E12-06-0492.
- 1014 **Fendrych, M., Synek, L., Pecenkova, T., Toupalova, H., Cole, R., Drdova, E.,**
 1015 **Nebesarova, J., Sedinova, M., Hala, M., Fowler, J.E., et al.** (2010). The
 1016 *Arabidopsis* exocyst complex is involved in cytokinesis and cell plate maturation.
 1017 *Plant Cell* **22**:3053-3065. 10.1105/tpc.110.074351.
- 1018 **Feng, S., Knodler, A., Ren, J., Zhang, J., Zhang, X., Hong, Y., Huang, S.,**
 1019 **Peranen, J., and Guo, W.** (2012). A Rab8 guanine nucleotide exchange factor-
 1020 effector interaction network regulates primary ciliogenesis. *J Biol Chem* **287**:15602-
 1021 15609. 10.1074/jbc.M111.333245.
- 1022 **Feraru, E., Feraru, M.I., Asaoka, R., Paciorek, T., De Rycke, R., Tanaka, H.,**
 1023 **Nakano, A., and Friml, J.** (2012). BEX5/RabA1b regulates trans-Golgi network-to-
 1024 plasma membrane protein trafficking in *Arabidopsis*. *Plant Cell* **24**:3074-3086.
 1025 10.1105/tpc.112.098152.
- 1026 **French, A.P., Mills, S., Swarup, R., Bennett, M.J., and Pridmore, T.P.** (2008).
 1027 Colocalization of fluorescent markers in confocal microscope images of plant cells.
 1028 *Nat Protoc* **3**:619-628. 10.1038/nprot.2008.31.
- 1029 **Friml, J., Benkova, E., Blilou, I., Wisniewska, J., Hamann, T., Ljung, K., Woody,**
 1030 **S., Sandberg, G., Scheres, B., Jurgens, G., et al.** (2002). AtPIN4 mediates sink-
 1031 driven auxin gradients and root patterning in *Arabidopsis*. *Cell* **108**:661-673.
 1032 10.1016/s0092-8674(02)00656-6.
- 1033 **Fujiwara, M., Uemura, T., Ebine, K., Nishimori, Y., Ueda, T., Nakano, A., Sato,**
 1034 **M.H., and Fukao, Y.** (2014). Interactomics of Qa-SNARE in *Arabidopsis thaliana*.
 1035 *Plant Cell Physiol* **55**:781-789. 10.1093/pcp/pcu038.
- 1036 **Geldner, N., Denervaud-Tendon, V., Hyman, D.L., Mayer, U., Stierhof, Y.D., and**

- 1037 **Chory, J.** (2009). Rapid, combinatorial analysis of membrane compartments in intact
 1038 plants with a multicolor marker set. *Plant J* **59**:169-178. 10.1111/j.1365-
 1039 313X.2009.03851.x.
- 1040 **Gerdes, H.H.** (2008). Membrane traffic in the secretory pathway. *Cell Mol Life Sci*
 1041 **65**:2779-2780. 10.1007/s00018-008-8348-z.
- 1042 **Grefen, C., and Blatt, M.R.** (2012). A 2in1 cloning system enables ratiometric
 1043 bimolecular fluorescence complementation (rBiFC). *Biotechniques* **53**:311-314.
 1044 10.2144/000113941.
- 1045 **Grefen, C., Chen, Z., Honsbein, A., Donald, N., Hills, A., and Blatt, M.R.** (2010a).
 1046 A novel motif essential for SNARE interaction with the K(+) channel KC1 and
 1047 channel gating in Arabidopsis. *Plant Cell* **22**:3076-3092. 10.1105/tpc.110.077768.
- 1048 **Grefen, C., Donald, N., Hashimoto, K., Kudla, J., Schumacher, K., and Blatt,
 1049 M.R.** (2010b). A ubiquitin-10 promoter-based vector set for fluorescent protein
 1050 tagging facilitates temporal stability and native protein distribution in transient and
 1051 stable expression studies. *Plant J* **64**:355-365. 10.1111/j.1365-313X.2010.04322.x.
- 1052 **Guo, W., Roth, D., Walch-Solimena, C., and Novick, P.** (1999). The exocyst is an
 1053 effector for Sec4p, targeting secretory vesicles to sites of exocytosis. *EMBO J*
 1054 **18**:1071-1080. 10.1093/emboj/18.4.1071.
- 1055 **Hala, M., Cole, R., Synek, L., Drdova, E., Pecenkova, T., Nordheim, A.,
 1056 Lamkemeyer, T., Madlung, J., Hochholdinger, F., Fowler, J.E., et al.** (2008). An
 1057 exocyst complex functions in plant cell growth in Arabidopsis and tobacco. *Plant Cell*
 1058 **20**:1330-1345. 10.1105/tpc.108.059105.
- 1059 **He, B., and Guo, W.** (2009). The exocyst complex in polarized exocytosis. *Curr Opin
 1060 Cell Biol* **21**:537-542. 10.1016/j.ceb.2009.04.007.
- 1061 **He, B., Xi, F., Zhang, X., Zhang, J., and Guo, W.** (2007). Exo70 interacts with

- 1062 phospholipids and mediates the targeting of the exocyst to the plasma membrane.
 1063 EMBO J **26**:4053-4065. 10.1038/sj.emboj.7601834.
- 1064 **Heard, W., Sklenar, J., Tome, D.F., Robatzek, S., and Jones, A.M.** (2015).
 1065 Identification of Regulatory and Cargo Proteins of Endosomal and Secretory
 1066 Pathways in *Arabidopsis thaliana* by Proteomic Dissection. Mol Cell Proteomics
 1067 **14**:1796-1813. 10.1074/mcp.M115.050286.
- 1068 **Heider, M.R., and Munson, M.** (2012). Exorcising the exocyst complex. Traffic
 1069 **13**:898-907. 10.1111/j.1600-0854.2012.01353.x.
- 1070 **Honsbein, A., Sokolovski, S., Grefen, C., Campanoni, P., Pratelli, R., Paneque,**
 1071 **M., Chen, Z., Johansson, I., and Blatt, M.R.** (2009). A tripartite SNARE-K+
 1072 channel complex mediates in channel-dependent K+ nutrition in *Arabidopsis*. Plant
 1073 Cell **21**:2859-2877. 10.1105/tpc.109.066118.
- 1074 **Ichikawa, M., Hirano, T., Enami, K., Fuselier, T., Kato, N., Kwon, C., Voigt, B.,**
 1075 **Schulze-Lefert, P., Baluska, F., and Sato, M.H.** (2014). Syntaxin of plant proteins
 1076 SYP123 and SYP132 mediate root hair tip growth in *Arabidopsis thaliana*. Plant Cell
 1077 Physiol **55**:790-800. 10.1093/pcp/pcu048.
- 1078 **Jin, Y., Sultana, A., Gandhi, P., Franklin, E., Hamamoto, S., Khan, A.R.,**
 1079 **Munson, M., Schekman, R., and Weisman, L.S.** (2011). Myosin V transports
 1080 secretory vesicles via a Rab GTPase cascade and interaction with the exocyst
 1081 complex. Dev Cell **21**:1156-1170. 10.1016/j.devcel.2011.10.009.
- 1082 **Jonsson, K., Boutte, Y., Singh, R.K., Gendre, D., and Bhalerao, R.P.** (2017).
 1083 Ethylene Regulates Differential Growth via BIG ARF-GEF-Dependent Post-Golgi
 1084 Secretory Trafficking in *Arabidopsis*. Plant Cell **29**:1039-1052. 10.1105/tpc.16.00743.
- 1085 **Karnik, R., Grefen, C., Bayne, R., Honsbein, A., Kohler, T., Kioumourtzoglou,**
 1086 **D., Williams, M., Bryant, N.J., and Blatt, M.R.** (2013). *Arabidopsis* Sec1/Munc18
 1087 protein SEC11 is a competitive and dynamic modulator of SNARE binding and

- 1088 SYP121-dependent vesicle traffic. *Plant Cell* **25**:1368-1382. 10.1105/tpc.112.108506.
- 1089 **Knodler, A., Feng, S., Zhang, J., Zhang, X., Das, A., Peranen, J., and Guo, W.**
 1090 (2010). Coordination of Rab8 and Rab11 in primary ciliogenesis. *Proc Natl Acad Sci
 1091 U S A* **107**:6346-6351. 10.1073/pnas.1002401107.
- 1092 **Kulich, I., Pecenkova, T., Sekeres, J., Smetana, O., Fendrych, M., Foissner, I.,
 1093 Hoftberger, M., and Zarsky, V.** (2013). Arabidopsis exocyst subcomplex containing
 1094 subunit EXO70B1 is involved in autophagy-related transport to the vacuole. *Traffic*
 1095 **14**:1155-1165. 10.1111/tra.12101.
- 1096 **Kwon, C., Neu, C., Pajonk, S., Yun, H.S., Lipka, U., Humphry, M., Bau, S.,
 1097 Straus, M., Kwaaitaal, M., Rampelt, H., et al.** (2008). Co-option of a default
 1098 secretory pathway for plant immune responses. *Nature* **451**:835-840.
 1099 10.1038/nature06545.
- 1100 **Larson, E.R., Ortmannova, J., Donald, N.A., Alvim, J., Blatt, M.R., and Zarsky,
 1101 V.** (2020). Synergy among Exocyst and SNARE Interactions Identifies a Functional
 1102 Hierarchy in Secretion during Vegetative Growth. *Plant Cell* **32**:2951-2963.
 1103 10.1105/tpc.20.00280.
- 1104 **Li, J., Wu, W.H., and Wang, Y.** (2017a). Potassium channel AKT1 is involved in the
 1105 auxin-mediated root growth inhibition in Arabidopsis response to low K(+) stress. *J
 1106 Integr Plant Biol* **59**:895-909. 10.1111/jipb.12575.
- 1107 **Li, R., Rodriguez-Furlan, C., Wang, J., van de Ven, W., Gao, T., Raikhel, N.V.,
 1108 and Hicks, G.R.** (2017b). Different Endomembrane Trafficking Pathways Establish
 1109 Apical and Basal Polarities. *Plant Cell* **29**:90-108. 10.1105/tpc.16.00524.
- 1110 **Li, S., Chen, M., Yu, D., Ren, S., Sun, S., Liu, L., Ketelaar, T., Emons, A.M., and
 1111 Liu, C.M.** (2013). EXO70A1-mediated vesicle trafficking is critical for tracheary
 1112 element development in Arabidopsis. *Plant Cell* **25**:1774-1786.
 1113 10.1105/tpc.113.112144.

- 1114 **Lin, Y., Ding, Y., Wang, J., Shen, J., Kung, C.H., Zhuang, X., Cui, Y., Yin, Z., Xia, Y., Lin, H., et al.** (2015). Exocyst-Positive Organelles and Autophagosomes Are
 1115 Distinct Organelles in Plants. *Plant Physiol* **169**:1917-1932. 10.1104/pp.15.00953.
- 1117 **Liu, J., and Guo, W.** (2012). The exocyst complex in exocytosis and cell migration.
 1118 *Protoplasma* **249**:587-597. 10.1007/s00709-011-0330-1.
- 1119 **Luo, G., Zhang, J., and Guo, W.** (2014). The role of Sec3p in secretory vesicle
 1120 targeting and exocyst complex assembly. *Mol Biol Cell* **25**:3813-3822.
 1121 10.1091/mbc.E14-04-0907.
- 1122 **Mao, H., Nakamura, M., Viotti, C., and Grebe, M.** (2016). A Framework for
 1123 Lateral Membrane Trafficking and Polar Tethering of the PEN3 ATP-Binding Cassette
 1124 Transporter. *Plant Physiol* **172**:2245-2260. 10.1104/pp.16.01252.
- 1125 **Mayers, J.R., Hu, T., Wang, C., Cardenas, J.J., Tan, Y., Pan, J., and Bednarek, S.Y.** (2017). SCD1 and SCD2 Form a Complex That Functions with the Exocyst and
 1126 RabE1 in Exocytosis and Cytokinesis. *Plant Cell* **29**:2610-2625.
 1127 10.1105/tpc.17.00409.
- 1129 **Mei, K., and Guo, W.** (2018). The exocyst complex. *Curr Biol* **28**:R922-R925.
 1130 10.1016/j.cub.2018.06.042.
- 1131 **Mima, J., and Wickner, W.** (2009). Phosphoinositides and SNARE chaperones
 1132 synergistically assemble and remodel SNARE complexes for membrane fusion. *Proc
 1133 Natl Acad Sci U S A* **106**:16191-16196. 10.1073/pnas.0908694106.
- 1134 **Morgera, F., Sallah, M.R., Dubuke, M.L., Gandhi, P., Brewer, D.N., Carr, C.M., and Munson, M.** (2012). Regulation of exocytosis by the exocyst subunit Sec6 and
 1135 the SM protein Sec1. *Mol Biol Cell* **23**:337-346. 10.1091/mbc.E11-08-0670.
- 1137 **Mukherjee, D., Sen, A., and Aguilar, R.C.** (2014). RhoGTPase-binding proteins, the
 1138 exocyst complex and polarized vesicle trafficking. *Small GTPases* **5**:e28453.

- 1139 10.4161/sgtp.28453.
- 1140 **Nielsen, E., Cheung, A.Y., and Ueda, T.** (2008). The regulatory RAB and ARF
1141 GTPases for vesicular trafficking. *Plant Physiol* **147**:1516-1526.
1142 10.1104/pp.108.121798.
- 1143 **Ortiz, D., Medkova, M., Walch-Solimena, C., and Novick, P.** (2002). Ypt32 recruits
1144 the Sec4p guanine nucleotide exchange factor, Sec2p, to secretory vesicles; evidence
1145 for a Rab cascade in yeast. *J Cell Biol* **157**:1005-1015. 10.1083/jcb.200201003.
- 1146 **Ory, S., and Gasman, S.** (2011). Rho GTPases and exocytosis: what are the
1147 molecular links? *Semin Cell Dev Biol* **22**:27-32. 10.1016/j.semcd.2010.12.002.
- 1148 **Oztan, A., Silvis, M., Weisz, O.A., Bradbury, N.A., Hsu, S.C., Goldenring, J.R.,
1149 Yeaman, C., and Apodaca, G.** (2007). Exocyst requirement for endocytic traffic
1150 directed toward the apical and basolateral poles of polarized MDCK cells. *Mol Biol
1151 Cell* **18**:3978-3992. 10.1091/mbc.e07-02-0097.
- 1152 **Pecenkova, T., Hala, M., Kulich, I., Kocourkova, D., Drdova, E., Fendrych, M.,
1153 Toupalova, H., and Zarsky, V.** (2011). The role for the exocyst complex subunits
1154 Exo70B2 and Exo70H1 in the plant-pathogen interaction. *J Exp Bot* **62**:2107-2116.
1155 10.1093/jxb/erq402.
- 1156 **Peng, J., Ilarslan, H., Wurtele, E.S., and Bassham, D.C.** (2011). AtRabD2b and
1157 AtRabD2c have overlapping functions in pollen development and pollen tube growth.
1158 *Bmc Plant Biol* **11**:25. 10.1186/1471-2229-11-25.
- 1159 **Pereira-Leal, J.B., Hume, A.N., and Seabra, M.C.** (2001). Prenylation of Rab
1160 GTPases: molecular mechanisms and involvement in genetic disease. *FEBS Lett*
1161 **498**:197-200. 10.1016/s0014-5793(01)02483-8.
- 1162 **Pinheiro, H., Samalova, M., Geldner, N., Chory, J., Martinez, A., and Moore, I.**
1163 (2009). Genetic evidence that the higher plant Rab-D1 and Rab-D2 GTPases exhibit

- 1164 distinct but overlapping interactions in the early secretory pathway. *J Cell Sci*
 1165 **122**:3749-3758. 10.1242/jcs.050625.
- 1166 **Preuss, M.L., Serna, J., Falbel, T.G., Bednarek, S.Y., and Nielsen, E.** (2004). The
 1167 Arabidopsis Rab GTPase RabA4b localizes to the tips of growing root hair cells. *Plant*
 1168 *Cell* **16**:1589-1603. 10.1105/tpc.021634.
- 1169 **Preuss, M.L., Schmitz, A.J., Thole, J.M., Bonner, H.K., Otegui, M.S., and**
 1170 **Nielsen, E.** (2006). A role for the RabA4b effector protein PI-4Kbeta1 in polarized
 1171 expansion of root hair cells in *Arabidopsis thaliana*. *J Cell Biol* **172**:991-998.
 1172 10.1083/jcb.200508116.
- 1173 **Rosquete, M.R., Davis, D.J., and Drakakaki, G.** (2018). The Plant Trans-Golgi
 1174 Network: Not Just a Matter of Distinction. *Plant Physiol* **176**:187-198.
 1175 10.1104/pp.17.01239.
- 1176 **Rutherford, S., and Moore, I.** (2002). The Arabidopsis Rab GTPase family: another
 1177 enigma variation. *Current Opinion in Plant Biology* **5**:518-528.
- 1178 **Safavian, D., Zayed, Y., Indriolo, E., Chapman, L., Ahmed, A., and Goring, D.R.**
 1179 (2015). RNA Silencing of Exocyst Genes in the Stigma Impairs the Acceptance of
 1180 Compatible Pollen in *Arabidopsis*. *Plant Physiol* **169**:2526-2538.
 1181 10.1104/pp.15.00635.
- 1182 **Speth, E.B., Imboden, L., Hauck, P., and He, S.Y.** (2009). Subcellular localization
 1183 and functional analysis of the Arabidopsis GTPase RabE. *Plant Physiol* **149**:1824-
 1184 1837. 10.1104/pp.108.132092.
- 1185 **Stegmann, M., Anderson, R.G., Ichimura, K., Pecenkova, T., Reuter, P., Zarsky,**
 1186 **V., McDowell, J.M., Shirasu, K., and Trujillo, M.** (2012). The ubiquitin ligase
 1187 PUB22 targets a subunit of the exocyst complex required for PAMP-triggered
 1188 responses in *Arabidopsis*. *Plant Cell* **24**:4703-4716. 10.1105/tpc.112.104463.

- 1189 **Stein, M., Dittgen, J., Sanchez-Rodriguez, C., Hou, B.H., Molina, A., Schulze-**
 1190 **Lefert, P., Lipka, V., and Somerville, S.** (2006). *Arabidopsis PEN3/PDR8*, an ATP
 1191 binding cassette transporter, contributes to nonhost resistance to inappropriate
 1192 pathogens that enter by direct penetration. *Plant Cell* **18**:731-746.
 1193 10.1105/tpc.105.038372.
- 1194 **Stenmark, H.** (2009). Rab GTPases as coordinators of vesicle traffic. *Nat Rev Mol*
 1195 *Cell Biol* **10**:513-525. 10.1038/nrm2728.
- 1196 **Sultana, A., Jin, Y., Dregger, C., Franklin, E., Weisman, L.S., and Khan, A.R.**
 1197 (2011). The activation cycle of Rab GTPase Ypt32 reveals structural determinants of
 1198 effector recruitment and GDI binding. *FEBS Lett* **585**:3520-3527.
 1199 10.1016/j.febslet.2011.10.013.
- 1200 **Synek, L., Schlager, N., Elias, M., Quentin, M., Hauser, M.T., and Zarsky, V.**
 1201 (2006). AtEXO70A1, a member of a family of putative exocyst subunits specifically
 1202 expanded in land plants, is important for polar growth and plant development. *Plant J*
 1203 **48**:54-72. 10.1111/j.1365-313X.2006.02854.x.
- 1204 **Synek, L., Vukasinovic, N., Kulich, I., Hala, M., Aldorfova, K., Fendrych, M.,**
 1205 **and Zarsky, V.** (2017). EXO70C2 Is a Key Regulatory Factor for Optimal Tip
 1206 Growth of Pollen. *Plant Physiol* **174**:223-240. 10.1104/pp.16.01282.
- 1207 **Synek, L., Pleskot, R., Sekeres, J., Serrano, N., Vukasinovic, N., Ortmannova, J.,**
 1208 **Klejchova, M., Pejchar, P., Batystova, K., Gutkowska, M., et al.** (2021). Plasma
 1209 membrane phospholipid signature recruits the plant exocyst complex via the
 1210 EXO70A1 subunit. *Proc Natl Acad Sci U S A* **118**10.1073/pnas.2105287118.
- 1211 **Szumlanski, A.L., and Nielsen, E.** (2009). The Rab GTPase RabA4d regulates pollen
 1212 tube tip growth in *Arabidopsis thaliana*. *Plant Cell* **21**:526-544.
 1213 10.1105/tpc.108.060277.
- 1214 **Takemoto, K., Ebine, K., Askani, J.C., Kruger, F., Gonzalez, Z.A., Ito, E., Goh,**

- 1215 **T., Schumacher, K., Nakano, A., and Ueda, T.** (2018). Distinct sets of tethering
 1216 complexes, SNARE complexes, and Rab GTPases mediate membrane fusion at the
 1217 vacuole in Arabidopsis. *Proc Natl Acad Sci U S A* **115**:E2457-E2466.
 1218 10.1073/pnas.1717839115.
- 1219 **Vernoud, V., Horton, A.C., Yang, Z., and Nielsen, E.** (2003). Analysis of the small
 1220 GTPase gene superfamily of Arabidopsis. *Plant Physiol* **131**:1191-1208.
 1221 10.1104/pp.013052.
- 1222 **Vukasinovic, N., and Zarsky, V.** (2016). Tethering Complexes in the Arabidopsis
 1223 Endomembrane System. *Front Cell Dev Biol* **4**:46. 10.3389/fcell.2016.00046.
- 1224 **Wang, J., Ding, Y., Wang, J., Hillmer, S., Miao, Y., Lo, S.W., Wang, X., Robinson,
 1225 D.G., and Jiang, L.** (2010). EXPO, an exocyst-positive organelle distinct from
 1226 multivesicular endosomes and autophagosomes, mediates cytosol to cell wall
 1227 exocytosis in Arabidopsis and tobacco cells. *Plant Cell* **22**:4009-4030.
 1228 10.1105/tpc.110.080697.
- 1229 **Wang, W., Liu, N., Gao, C., Cai, H., Romeis, T., and Tang, D.** (2020). The
 1230 Arabidopsis exocyst subunits EXO70B1 and EXO70B2 regulate FLS2 homeostasis at
 1231 the plasma membrane. *New Phytol* **227**:529-544. 10.1111/nph.16515.
- 1232 **Wang, X., Chung, K.P., Lin, W., and Jiang, L.** (2017). Protein secretion in plants:
 1233 conventional and unconventional pathways and new techniques. *J Exp Bot* **69**:21-37.
 1234 10.1093/jxb/erx262.
- 1235 **Wattelet-Boyer, V., Brocard, L., Jonsson, K., Esnay, N., Joubes, J., Domergue, F.,
 1236 Mongrand, S., Raikhel, N., Bhalerao, R.P., Moreau, P., et al.** (2016). Enrichment
 1237 of hydroxylated C24- and C26-acyl-chain sphingolipids mediates PIN2 apical sorting
 1238 at trans-Golgi network subdomains. *Nat Commun* **7**:12788. 10.1038/ncomms12788.
- 1239 **Welz, T., Wellbourne-Wood, J., and Kerkhoff, E.** (2014). Orchestration of cell
 1240 surface proteins by Rab11. *Trends Cell Biol* **24**:407-415. 10.1016/j.tcb.2014.02.004.

- 1241 **Wu, B., and Guo, W.** (2015). The Exocyst at a Glance. *J Cell Sci* **128**:2957-2964.
 1242 10.1242/jcs.156398.
- 1243 **Wu, C., Tan, L., van Hooren, M., Tan, X., Liu, F., Li, Y., Zhao, Y., Li, B., Rui, Q.,**
 1244 **Munnik, T., et al.** (2017). Arabidopsis EXO70A1 recruits Patellin3 to the cell
 1245 membrane independent of its role as an exocyst subunit. *J Integr Plant Biol* **59**:851-
 1246 865. 10.1111/jipb.12578.
- 1247 **Wu, H., Rossi, G., and Brennwald, P.** (2008). The ghost in the machine: small
 1248 GTPases as spatial regulators of exocytosis. *Trends Cell Biol* **18**:397-404.
 1249 10.1016/j.tcb.2008.06.007.
- 1250 **Wu, S., Mehta, S.Q., Pichaud, F., Bellen, H.J., and Quiroga, F.A.** (2005). Sec15
 1251 interacts with Rab11 via a novel domain and affects Rab11 localization in vivo. *Nat*
 1252 Struct Mol Biol **12**:879-885. 10.1038/nsmb987.
- 1253 **Xu, J., and Scheres, B.** (2005). Dissection of Arabidopsis ADP-RIBOSYLATION
 1254 FACTOR 1 function in epidermal cell polarity. *Plant Cell* **17**:525-536.
 1255 10.1105/tpc.104.028449.
- 1256 **Zarsky, V., Kulich, I., Fendrych, M., and Pecenkova, T.** (2013). Exocyst complexes
 1257 multiple functions in plant cells secretory pathways. *Curr Opin Plant Biol* **16**:726-733.
 1258 10.1016/j.pbi.2013.10.013.
- 1259 **Zhang, B., Karnik, R., Waghmare, S., Donald, N., and Blatt, M.R.** (2017).
 1260 VAMP721 Conformations Unmask an Extended Motif for K⁺ Channel Binding and
 1261 Gating Control. *Plant Physiol* **173**:536-551. 10.1104/pp.16.01549.
- 1262 **Zhang, L., Ma, J., Liu, H., Yi, Q., Wang, Y., Xing, J., Zhang, P., Ji, S., Li, M., Li,
 1263 J., et al.** (2021). SNARE proteins VAMP721 and VAMP722 mediate the post-Golgi
 1264 trafficking required for auxin-mediated development in Arabidopsis. *Plant J*
 1265 10.1111/tpj.15450.

- 1266 **Zhang, X., Hu, Z., Guo, Y., Shan, X., Li, X., and Lin, J.** (2020). High-efficiency
1267 procedure to characterize, segment, and quantify complex multicellularity in raw
1268 micrographs in plants. *Plant Methods* **16**:100. 10.1186/s13007-020-00642-0.
- 1269 **Zhang, X., Cui, Y., Yu, M., Su, B., Gong, W., Baluska, F., Komis, G., Samaj, J.,**
1270 **Shan, X., and Lin, J.** (2019). Phosphorylation-Mediated Dynamics of Nitrate
1271 Transceptor NRT1.1 Regulate Auxin Flux and Nitrate Signaling in Lateral Root
1272 Growth. *Plant Physiol* **181**:480-498. 10.1104/pp.19.00346.
- 1273 **Zhang, X.M., Ellis, S., Sriratana, A., Mitchell, C.A., and Rowe, T.** (2004). Sec15 is
1274 an effector for the Rab11 GTPase in mammalian cells. *J Biol Chem* **279**:43027-43034.
1275 10.1074/jbc.M402264200.
- 1276 **Zhang, Y., Liu, C.M., Emons, A.M., and Ketelaar, T.** (2010). The plant exocyst. *J*
1277 *Integr Plant Biol* **52**:138-146. 10.1111/j.1744-7909.2010.00929.x.
- 1278 **Zhang, Y., Immink, R., Liu, C.M., Emons, A.M., and Ketelaar, T.** (2013). The
1279 Arabidopsis exocyst subunit SEC3A is essential for embryo development and
1280 accumulates in transient puncta at the plasma membrane. *New Phytol* **199**:74-88.
1281 10.1111/nph.12236.
- 1282 **Zhao, T., Rui, L., Li, J., Nishimura, M.T., Vogel, J.P., Liu, N., Liu, S., Zhao, Y.,**
1283 **Dangl, J.L., and Tang, D.** (2015). A truncated NLR protein, TIR-NBS2, is required
1284 for activated defense responses in the exo70B1 mutant. *PLoS Genet* **11**:e1004945.
1285 10.1371/journal.pgen.1004945.
- 1286
- 1287
- 1288
- 1289
- 1290
- 1291
- 1292

1293 **Figure Legends**

1294 **Figure 1. SNARE proteins VAMP721 and SYP121 are downstream effectors of**
 1295 **RABA2a.**

1296 **(A)** *In vivo* coimmunoprecipitation (co-IP) assay demonstrates that the SNARE
 1297 proteins VAMP721 and SYP121 co-precipitate with YFP-RABA2a but not with YFP-
 1298 RABC1 or YFP-RABD2b. Protein samples were extracted from 7-day-old transgenic
 1299 seedlings harboring transgenes *pUBQ10::YFP*, *YFP-RABA2a*, *YFP-RABC1* or *YFP-*
 1300 *RABD2b* and probed by immunoblot. Ponceau S staining of ribulose-1,5-bis-
 1301 phosphate carboxylase/oxygenase (Rubisco) bands is included as loading control
 1302 (bottom). Molecular weight markers are in kD.

1303 **(B and C)** Split-ubiquitin yeast two-hybrid (SU-Y2H) assays show that RABA2aΔC
 1304 interacts with VAMP721 **(B)** and SYP121 **(C)** specifically in its GTP-bound state.
 1305 **(D)** Active RABA2aΔC interacts with VAMP722 but not VAMP723, VAMP726 or
 1306 VAMP727.

1307 **(E)** Active RABA2aΔC also interacts with SYP122 but not SYP123, SYP124 or
 1308 SYP125.

1309 **(F, G)** Schematic representation of the *pBiFCt-2in1-NN* polycistronic vectors used in
 1310 bimolecular fluorescence complementation (BiFC) assay.

1311 **(H, I)** BiFC assay supports the interaction of RABA2aΔC in its GTP-bound state with
 1312 VAMP721 **(H)** and SYP121 **(I)** and the lack of interaction with VAMP723 **(H)** or
 1313 SYP123 **(I)**. RFP fluorescence was set as the internal control. *cYFP* with the empty
 1314 cassette was used as negative control. Scale bars = 50 μm.

1315 **(J, K)** Quantification of the fluorescence ratio between YFP and RFP in different
 1316 BiFC assays mentioned in **H** and **I**.

1317 Images are representative of at least three biological repeats. For **J** and **K**, values are
 1318 means ± SE ($n = 20\text{--}25$). Statistically significant differences ($P < 0.05$) were
 1319 determined using Tukey's multiple comparison in ANOVA.

1320

1321 **Figure 2. RABA2a affects the assembly of the VAMP721-SYP121-SNAP33**
 1322 **SNARE complex.**

1323 **(A and B)** RABA2a colocalizes with VAMP721 (**A**) or SYP121 (**B**) in the same
 1324 subcellular compartments. Arrowheads indicate the co-localized foci. The Pearson
 1325 correlation coefficient (Rp) and Spearman correlation coefficient (Rs) are indicated on
 1326 the scatterplots of each representative image.

1327 **(C)** Schematic maps of the *pBiFCt-2in1-NN* and *pUBQ10::CFP-DEST* vectors used
 1328 in the competition assay.

1329 **(D and E)** Competition assay in *N. benthamiana* leaves showed that overexpression
 1330 of *RABA2a(Q71L)* enhances the YFP signal reconstructed by the SNARE pairs
 1331 SYP121 and VAMP721 (**D**), or SNAP33 and VAMP721 (**E**), whereas overexpression
 1332 of *RABA2a(S26N)* inhibits the assembly of the SNARE complex (**D, E**).

1333 **(F and G)** Quantification of the fluorescence ratio between YFP and RFP in
 1334 competition assays as mentioned in **D** and **E**.

1335 **(H and I)** *In vivo* co-IP assay revealed that overexpression of *RABA2a(Q71L)* induced
 1336 by 5 µM β-estradiol for 24 h does not change the interaction between the SNARE
 1337 proteins SYP121 and VAMP721 (**H**) whereas overexpressing *RABA2a(S26N)*
 1338 significantly reduces the interaction between the SNARE proteins (**I**). Values indicate
 1339 average band intensity from three or four biological repeats.

1340 Images are representative of at least three biological repeats. For **A** and **B**, scale bars
 1341 represent 10 µm; for **D** and **E**, scale bars represent 50 µm. Values shown are means ±
 1342 SE; *n* = 40 – 46 (**A, B**); *n* = 30 – 39 (**F, G**). Statistically significant differences (*P* <
 1343 0.05) were determined using Tukey's multiple comparison in ANOVA (**F, G**).

1344

1345 **Figure 3. Exocyst subunits do not interact with RABA2a or the downstream**
 1346 **SNARE proteins.**

1347 **(A, B)** Split-ubiquitin yeast two-hybrid (SU-Y2H) assays show that the exocyst
 1348 subunits EXO70A1, EXO84b, and SEC15b do not interact with VAMP721 (**A**) or
 1349 SYP121 (**B**). The interactions of VAMP721 or SYP121 with RABA2a(Q71L)ΔC
 1350 were used as positive controls.

1351 **(C–F)** The exocyst subunits EXO70A1, EXO84b, and SEC15b do not interact with
 1352 RABA2a(Q71L)ΔC, VAMP721, or SYP121 in LCI assays. Interactions between

1353 VAMP721 and SYP121, VAMP721 and RABA2a(Q71L) Δ C, SYP121 and
 1354 RABA2a(Q71L) Δ C, and EXO84b and SEC15b were used as positive controls.
 1355 Dotted-circles indicate the places where the samples were injected.
 1356 **(G)** Schematic representation of the *pBiFCt-2in1-NN* polycistronic vector used in the
 1357 BiFC assay.
 1358 **(H)** BiFC assays show that the exocyst subunits EXO70A1, EXO84b, and SEC15b do
 1359 not interact with RABA2a(Q71L) Δ C or the downstream SNARE proteins.
 1360 Interactions between VAMP721 and SYP121, between RABA2a(Q71L) Δ C and
 1361 VAMP721, and between SEC15b and SEC10 were used as positive controls.
 1362 **(I)** *In vivo* co-IP assays show that the exocyst subunits SEC6, SEC8, and SEC15b do
 1363 not interact with RABA2a; VAMP721 and SYP121 do not interact with EXO70A1 or
 1364 EXO84b. The interactions of RABA2a with VAMP721 and SYP121, and the
 1365 interactions among different exocyst subunits were used as positive controls. Protein
 1366 samples were extracted from 7-day-old transgenic seedlings of *pUBQ10::YFP*, *YFP-*
 1367 *RABA2a*, *EXO70A1-GFP*, or *EXO84b-GFP* for immunoblot analysis.
 1368 **(J, K)** RABA2a does not interact with RABE1d or SCD1 in a co-IP assay. The
 1369 interactions between RABE1d and SEC15b or SEC8 and between SCD1 and
 1370 RABE1d were used as positive controls. Protein samples were extracted from 7-day-
 1371 old transgenic seedlings harboring *pUBQ10::YFP*, *SCD1-GFP* or *YFP-RABE1d* for
 1372 immunoblot analysis.
 1373 Images are representative of at least three biological repeats. Scale bar represents 50
 1374 μ m.
 1375
 1376 **Figure 4. The exocyst- and the RABA2a-SNAREs mediated secretory pathways**
 1377 **are largely independent.**
 1378 **(A, B)** Subcellular localization of SNARE proteins and exocyst subunits in the
 1379 background of the *XVE>>RFP-RABA2a(S26N)* transgenic line. Overexpression of
 1380 *RABA2a(S26N)* induced by 5 μ M β -estradiol for 24 h dramatically reduces PM
 1381 localization and causes intracellular aggregation of SYP121(first row) and
 1382 VAMP721(second row). By contrast, overexpression of *RABA2a(S26N)* does not

1383 affect the membrane distribution of EXO70A1(third row) or EXO84b (fourth row).
 1384 **(C)** Quantification of the fluorescence ratio between the PM and cytoplasm in
 1385 different genotypes, with or without β-estradiol induction, as mentioned in **A** and **B**.
 1386 **(D, E)** *In vivo* co-IP assay reveals that overexpression of *RABA2a(Q71L)* (**D**) or
 1387 *RABA2a(S26N)* (**E**) does not affect the assembly of the exocyst in a co-IP assay.
 1388 **(F)** The PM localization patterns of RABA2a (first row), RABA2a(Q71L) (second
 1389 row), and SYP121 (third row) are not significantly altered in the *exo84b* mutant.
 1390 However, VAMP721 (fourth row) reduces the PM distribution and increases the
 1391 intracellular signal in the same mutant.
 1392 **(G)** Quantification of the fluorescence ratio between the PM and cytoplasm in the
 1393 genotypes mentioned in **F**.
 1394 **(H)** Representative images showing the subcellular colocalization between RABA2a
 1395 and VAMP721 in wild type and the *exo84b* mutant.
 1396 **(I)** Comparison of the Pearson correlation coefficient (Rp) and Spearman correlation
 1397 coefficient (Rs) between RABA2a and VAMP721 in wild type and the *exo84b* mutant.
 1398 **(J, K)** *In vivo* co-IP assay reveals that the interaction of RABA2a with VAMP721 and
 1399 SYP121 (**J**) and of VAMP721 with SYP121 (**K**) is not significantly altered in the
 1400 *exo84b* mutant. RABA2a and SYP121 do not interact with the exocyst subunits
 1401 (negative control).
 1402 Images are representative of at least three biological repeats. Scale bars represent 10
 1403 μm. Values shown are means ± SE; $n = 16\text{--}22$ (**C**); $n = 20\text{--}22$ (**G**); $n = 20\text{--}25$ (**I**).
 1404 Statistically significant differences were determined using Student's *t*-tests ($***P <$
 1405 0.001). “ns” indicates no significant difference between groups.

1406
 1407 **Figure 5. Exocyst and RABA2a-SNARE proteins follow different trafficking**
 1408 **routes during secretory processes.**
 1409 **(A–C)** Representative spinning disc confocal (SDC) images show that VAMP721 foci
 1410 colocalize with RABA2a foci (**A**) but are distinct from the vesicles labeled by
 1411 EXO84b (**B**) or EXO70A1 (**C**) in root epidermal cells.
 1412 **(D–F)** Kymograph analysis reveals that VAMP721 foci co-migrate with RABA2a foci

1413 **(D)** but follow different trafficking routes from EXO84b (**E**) or EXO70A1 (**F**) foci.
 1414 **(G–I)** To quantify the co-movement, a line was drawn in the same position for the red
 1415 and green channels shown in **D–F** and the signal intensity of each pixel was plotted
 1416 against the relative distance in both channels.
 1417 **(J)** Pearson correlation coefficient between VAMP721 and RABA2a or between
 1418 VAMP721 and EXO70A1 or EXO84b at the surface of root epidermal cells.
 1419 Images are representative of three biological repeats. **(A–C)** Scale bar represents 10
 1420 μm. **(D–F)** Scale bar represents 10 s. Values shown are means ± SE; $n = 28\text{--}34$ **(J)**.
 1421 Statistically significant differences ($P < 0.05$) were determined using Tukey's multiple
 1422 comparison in ANOVA.

1423

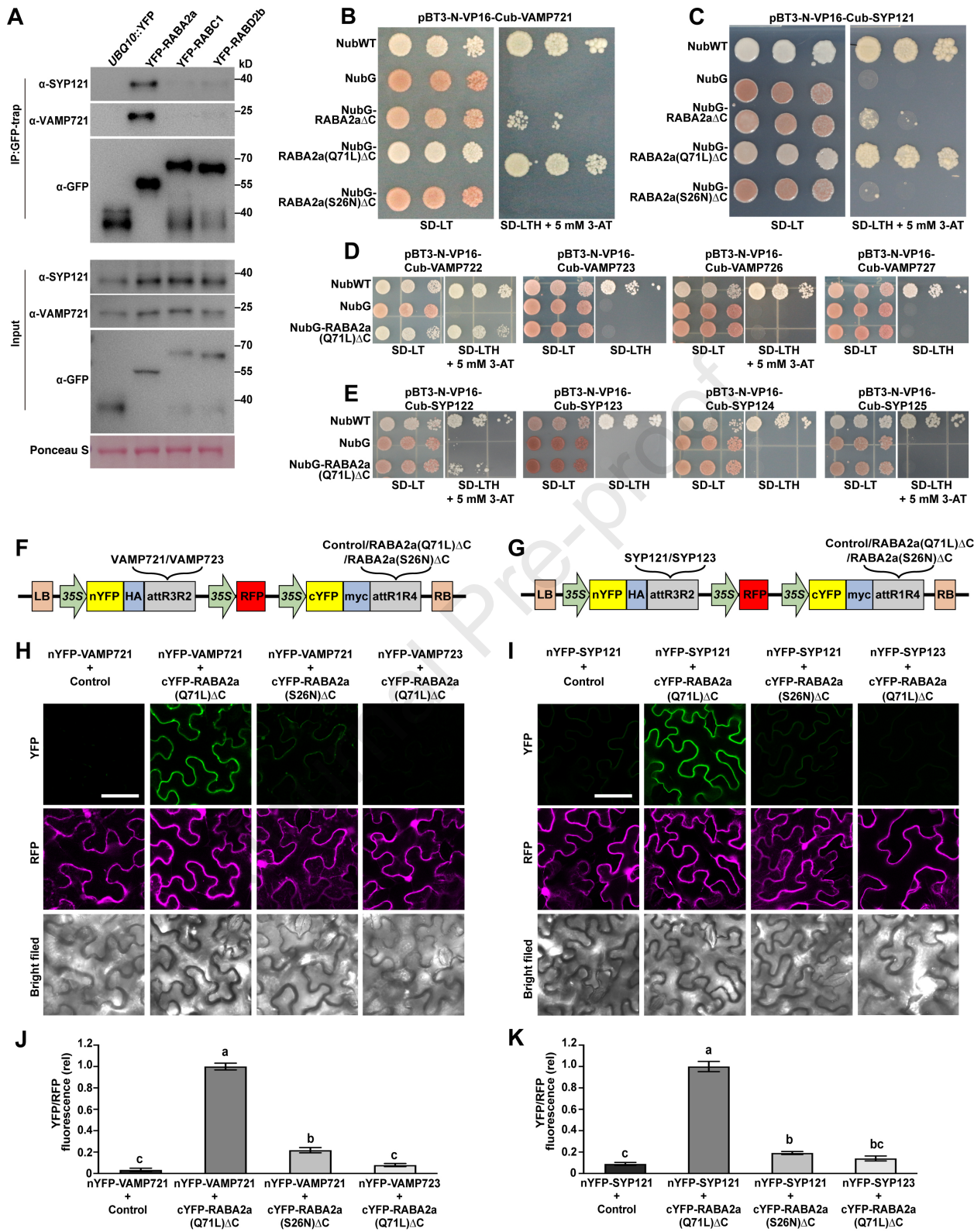
1424 **Figure 6. The exocyst and RABA2a-SNARE proteins select different cargos in**
 1425 **the secretory pathways.**

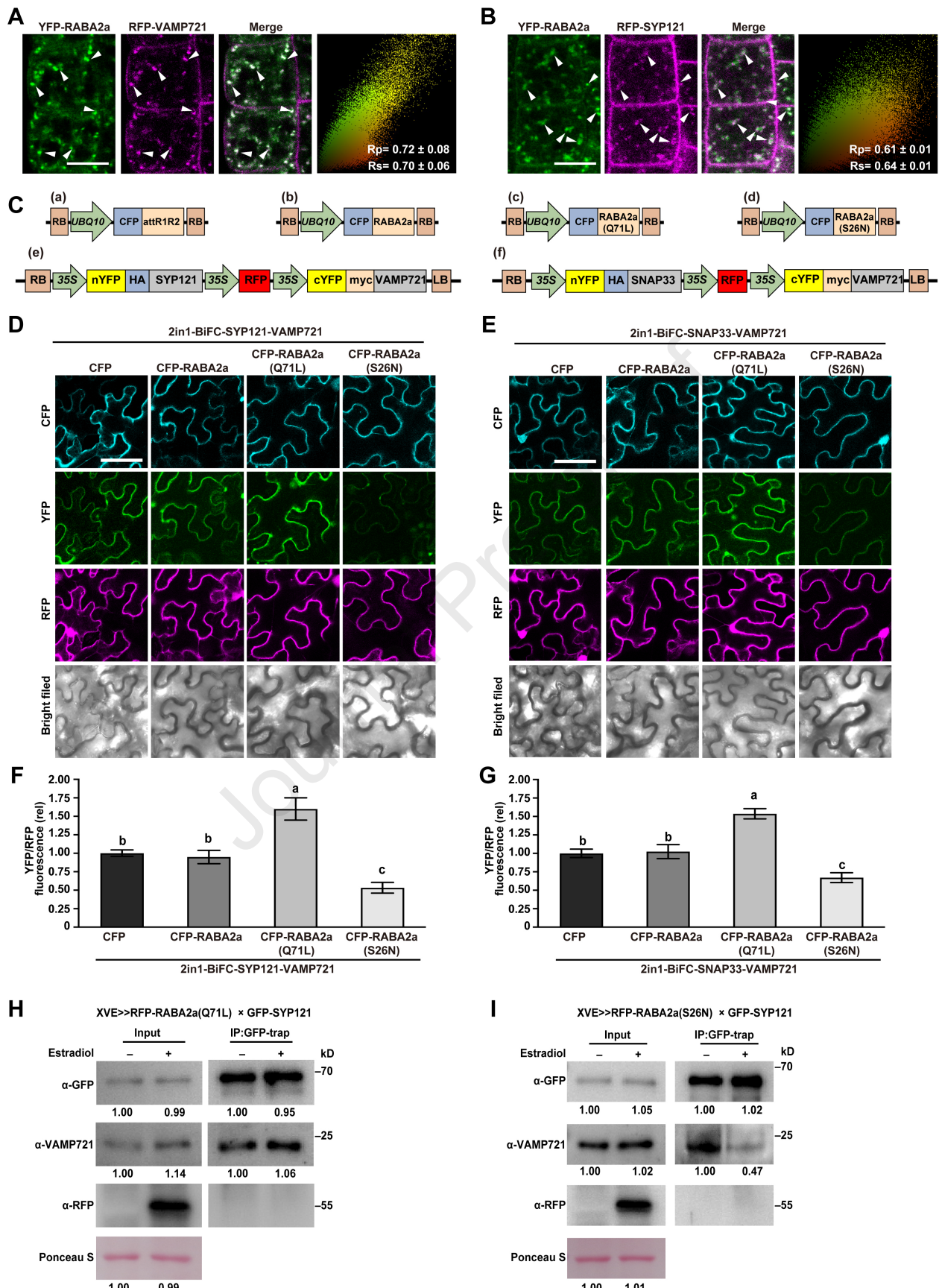
1426 **(A)** The PM localization of PEN3 (third column), but not PIN2 (first column) or PIN1
 1427 (second column), is reduced in the *exo84b* mutant.
 1428 **(B)** Quantification of the fluorescence ratio between the PM and cytoplasm in the
 1429 genotypes mentioned in **A**.
 1430 **(C, D)** Subcellular localization of cargo proteins in the *XVE>>RFP-RABA2a(S26N)*
 1431 transgenic line. Overexpression of *RABA2a(S26N)* induced by 5 μM β-estradiol for 24
 1432 h dramatically reduces the PM localization and causes the intracellular aggregation of
 1433 PIN2 (first row), but not PIN1 (second row) or PEN3 (third row).
 1434 **(E)** Quantification of the fluorescence ratio between the PM and cytoplasm in
 1435 different genotypes before and after β-estradiol induction as mentioned in **C** and **D**.
 1436 Images are representative of at least three biological repeats. Scale bars represent 10
 1437 μm. Values shown are means ± SE; $n = 20\text{--}25$ **(B)**; $n = 20\text{--}30$ **(E)**. Statistically
 1438 significant differences between groups were determined using Student's *t*-tests ($***P$
 1439 < 0.001). “ns” indicates no significant differences between groups.

1440

1441 **Figure 7. The physiological role of RABA2a-SNARE pathway and the working**
 1442 **model.**

1443 **(A)** Representative phenotype of 6-day-old wild type or seedlings overexpressing
1444 *RABA2a(Q71L)* or *RABA2a(S26N)* on MS medium (K⁺ concentrations: 18.7 mM/L)
1445 or MS medium lacking K⁺ (MS-K) supplemented with various KCl concentrations
1446 before and after induction by β-estradiol.
1447 **(B)** Protein accumulation levels of RABA2a(Q71L) or RABA2a(S26N) before and
1448 after induction by β-estradiol.
1449 **(C, D)** Relative root growth rate of wild type or seedlings overexpressing
1450 *RABA2a(Q71L)* or *RABA2a(S26N)* on MS medium or MS-K medium supplemented
1451 with various KCl concentrations before **(C)** and after **(D)** induction by β-estradiol.
1452 Images are representative of three biological repeats. Scale bar represents 1 cm.
1453 Values shown are means ± SE; *n* = 82–106 **(C, D)**. Statistically significant differences
1454 (*P* < 0.05) were determined using Tukey's multiple comparison in ANOVA.
1455 **(E)** Working model for the secretory pathways regulated by RABA2a-SNARE and the
1456 exocyst. At least two parallel pathways are proposed to function in plant cells during
1457 secretory processes. In the plant specific RABA2a-SNARE pathway, vesicles budding
1458 from the TGN bypass the tethering complex and fuse with the PM through an
1459 interaction with the SNARE complex. PIN2, an auxin effluxer, is the cargo protein in
1460 this pathway. In addition, the RABA2a-mediated secretory pathway also fine-tunes K⁺
1461 homeostasis, presumably by regulating the assembly of the SNARE complex. In a
1462 parallel pathway, exocyst-regulated exocytosis functions downstream of SCD1 and
1463 RABE1 proteins. PEN3 is transported to the PM through this pathway.
1464





Journal Pre-proof

